

A combined finite element and multiscale finite element method for the multiscale elliptic problems

Weibing Deng*

Haijun Wu†

Abstract

The oversampling multiscale finite element method (MsFEM) is one of the most popular methods for simulating composite materials and flows in porous media which may have many scales. But the method may be inapplicable or inefficient in some portions of the computational domain, e.g., near the domain boundary or near long narrow channels inside the domain due to the lack of permeability information outside of the domain or the fact that the high-conductivity features cannot be localized within a coarse-grid block. In this paper we develop a combined finite element and multiscale finite element method (FE-MsFEM), which deals with such portions by using the standard finite element method on a fine mesh and the other portions by the oversampling MsFEM. The transmission conditions across the FE-MSFE interface is treated by the penalty technique. A rigorous convergence analysis for this special FE-MsFEM is given under the assumption that the diffusion coefficient is periodic. Numerical experiments are carried out for the elliptic equations with periodic and random highly oscillating coefficients, as well as multiscale problems with high contrast channels, to demonstrate the accuracy and efficiency of the proposed method.

Key words. Multiscale problems, oversampling technique, interface penalty, combined finite element and multiscale finite element method

AMS subject classifications. 34E13, 35B27, 65N12, 65N15, 65N30

1 Introduction

Let $\Omega \subset \mathbb{R}^n$, $n = 2, 3$ be a polyhedral domain, and consider the following elliptic equation

$$(1.1) \quad \begin{cases} -\nabla \cdot (\mathbf{a}^\epsilon(x) \nabla u_\epsilon(x)) = f(x) & \text{in } \Omega, \\ u_\epsilon(x) = 0 & \text{on } \partial\Omega, \end{cases}$$

where $0 < \epsilon \ll 1$ is a parameter that represents the ratio of the smallest and largest scales in the problem, and $\mathbf{a}^\epsilon(x) = (a_{ij}^\epsilon(x))$ is a symmetric, positive definite, bounded tensor:

$$(1.2) \quad \lambda |\xi|^2 \leq a_{ij}^\epsilon(x) \xi_i \xi_j \leq \Lambda |\xi|^2 \quad \forall \xi \in \mathbb{R}^n, x \in \bar{\Omega}$$

for some positive constants λ and Λ .

*Department of Mathematics, Nanjing University, Jiangsu, 210093, P.R. China. (wbdeng@nju.edu.cn). The work of this author was partially supported by the the NSF of China grant 10971096 and by the Fundamental Research Funds for the Central Universities 1116020306.

†Department of Mathematics, Nanjing University, Jiangsu, 210093, P.R. China. (hjw@nju.edu.cn). The work of the second author was partially supported by the National Magnetic Confinement Fusion Science Program under grant 2011GB105003 and by the NSF of China grants 11071116, 91130004.

Problems of the type (1.1) are often used to describe the models arising from composite materials and flows in porous media, which contain many spatial scales. Solving these problems numerically is difficult because of that resolving the smallest scale in problems usually requires very fine meshes and hence tremendous amount of computer memory and CPU time. To overcome this difficulty, many methods have been designed to solve the problem on meshes that are coarser than the scale of oscillations. One of the most popular methods is the multiscale finite element method (MsFEM) [28, 42, 43], which takes its origin from the work of Babuška and Osborn [9, 8]. Two main ingredients of the MsFEM are the global formulation of the method such as various finite element methods and the construction of basis functions. The special basis functions which constructed from the local solutions of the elliptic operator contain the small scale information within each element. By solving the problem (1.1) in the special basis function space, they get a good approximation of the full fine scale solution. We remark that there are many other methods proposed to solve this type of multiscale problems in the past several decades. See, for instance, wavelet homogenization techniques [18, 30], multigrid numerical homogenization techniques [35, 50], the subgrid upscaling method [2, 3], the heterogeneous multiscale method [21, 22, 23], the residual-free bubble method (or the variational multiscale method, discontinuous enrichment method) [13, 31, 36, 37, 45, 54], mortar multiscale methods [4, 53], and upscaling or numerical homogenization method [20, 32, 59]. We refer the reader to the book [26] for an overview and more other references of multiscale numerical methods in the literature, especially a description of some intrinsic connections between most of these methods.

In this paper, we focus on the MsFEM. Many developments and extensions of the MsFEM have been done in the past ten years. See for example, the mixed MsFEM [14, 1], the MsFEMs for nonlinear problems [27, 29], the Petro-Galerkin MsFEM [44], the MsFEMs using limited global information [25, 51], and the multiscale finite volume method [46]. In [43], it is shown that there is a resonance error between the grid scale and the scales of the continuous problem. Especially, for the two-scale problem, the resonance error manifests as a ratio between the wavelength of the small scale oscillation and the grid size; the error becomes large when the two scales are close. The scale resonance is a fundamental difficulty caused by the mismatch between the local construction of the multiscale basis functions and the global nature of the elliptic problems. This mismatch between the local solution and the global solution produces a thin boundary layer in the first order corrector of the local solution. To overcome the difficulty due to the scale resonance, an oversampling technique was proposed in [42, 28]. The basic idea is computing the local problem in the domain with size larger than the mesh size H and use only the interior sampled information to construct the basis functions. By doing this, the influence of the boundary layer in the larger domain on the basis functions is greatly reduced.

However, for the coarse-grid elements near the boundary, in order to construct the multiscale basis functions, the oversampling MsFEM needs to assume that there is enough information available outside of the research domain, which is not applicable in practice.

To handle this problem, the natural way is to use the standard multiscale basis functions instead of the oversampling multiscale basis functions in the coarse-grid elements adjacent to the boundary, hence in this area we don't need to use the information outside the domain. We call this method as the mixed basis MsFEM. Since in the elements near the boundary, we use the multiscale basis functions without oversampling technique, the scale resonance comes out again hence pollute the accuracy.

To overcome this difficulty, we introduce a new method in this paper which can improve the accuracy significantly. The proposed method separates the research area into two sub-domains such that one of them is contained inside the domain with a distance away from the boundary. Then in the interior sub-domain the oversampling multiscale basis functions on a coarse mesh (with mesh size H) are used. While, in the other sub-domain which adjacent to the boundary the traditional linear FEM basis functions are used on a mesh (with mesh size h) which is fine enough to resolving multiscale features. The difficulty to realize this idea is how to joint the two methods together without losing accuracies of both methods, i.e., how to deal with the transmission condition on the interface between coarse and fine meshes efficiently. Thanks to the penalty techniques used in the interior penalty discontinuous (or continuous) Galerkin methods originated in 1970s [10, 11, 19, 56, 5, 6], we may deal with the transmission condition on the interface by penalizing the jumps from the function values as well as the fluxes of the finite element solution on the fine mesh to those of the oversampling multiscale finite element solution on the coarse mesh. A rigorous and careful analysis is given for the elliptic equation with periodic diffusion coefficient to show that the H^1 -error of our new method is just the sum of interpolation errors of both methods plus an error term of $O(\frac{H^2}{\sqrt{\epsilon}})$ introduced by the penalty terms, where H is the mesh size of the coarse mesh. We would like to remark that besides the applications of penalty technique to the interior penalty discontinuous (or continuous) Galerkin methods, this technique is also applied to the Helmholtz equation with high wave number to reduce the pollution error [33, 34, 57, 60] and applied to the interface problems to construct high order unfitted mesh methods[48, 58].

The other potential application of our proposed method is to solve the multiscale problems which may have some singularities. For example, the multiscale problem with Dirac function singularities, which stems from the simulation of steady flow transport through highly heterogeneous porous media driven by extraction wells [16], or the multiscale problems with high-conductivity channels that connect the boundaries of coarse-grid blocks [38, 39, 24, 52]. Our new FE-MsFEM may solve such problems by using the traditional FEM on a fine mesh near the singularities (and, of course, near the domain boundary) and using the oversampling MsFEM in the other part of the domain. To demonstrate the performance of the FE-MsFEM, we try to simulate multiscale elliptic problems which have fine and long-ranged high-conductivity channels. We remark that this kind of high-conductivity features cannot be localized within a coarse-grid block, hence it is difficult to be handled with standard or oversampling multiscale basis. The numerical results show that the introduced FE-MsFEM can solve the high contrast multiscale elliptic problems efficiently. The convergence analysis for multiscale problems with singularities and ap-

plications of the proposed FE-MsFEM to practical problems such as two-phase flows in porous media and other types of equations are currently under study.

The rest of this paper is organized as follows. In Section 2, we formulate the FE-MsFEM for the model problem. In Section 3, we review some classical homogenization results for the elliptic problems and give an interior H^2 norm error estimate between the multiscale solution and the homogenized solution with first order corrector. In Section 4, we give some approximation properties for the oversampling MsFE space and the linear FE space, respectively. The H^1 error estimate of the introduced FE-MsFEM is given in Section 5. In Section 6 we first give some numerical examples for both periodic and randomly generated coefficients to demonstrate the accuracy the proposed method, and then apply our method to multiscale elliptic problems which have fine and long-ranged high-conductivity channels to demonstrate the efficiency of the method. Conclusions are drawn in the last section.

Before leaving this section, we fix some notations and conventions to be used in this paper. In the following, the Einstein summation convention is used: summation is taken over repeated indices. $L^2(\Omega)$ denotes the space of square integrable functions defined in domain Ω . We use the $L^2(\Omega)$ based Sobolev spaces $H^k(\Omega)$ equipped with norms and seminorms given by:

$$\|u\|_{H^k(\Omega)}^2 = \int_{\Omega} \sum_{|\alpha| \leq k} |D^\alpha u|^2, \quad |u|_{H^k(\Omega)}^2 = \int_{\Omega} \sum_{|\alpha|=k} |D^\alpha u|^2.$$

$\|u\|_{W^{k,\infty}(\Omega)}$ ($|u|_{W^{k,\infty}(\Omega)}$) is the $W^{k,\infty}$ norm (seminorm) of u in Ω . Throughout, C, C_1, C_2, \dots denote generic constants, which are independent of ϵ, H and h unless otherwise stated. We also use the shorthand notation $A \lesssim B$ and $B \gtrsim A$ for the inequality $A \leq CB$ and $B \geq CA$. The notation $A \approx B$ is equivalent to the statement $A \lesssim B$ and $B \lesssim A$.

2 FE-MsFEM Formulation

In this section we present our FE-MsFEM. We describe the method only for the case of dealing with the difficulty of lack information outside the domain in the oversampling MsFEM. Of course, the formulation can easily be extended to the case of dealing with singularities.

We first separate the research area Ω into two sub-domains Ω_1 and Ω_2 such that $\Omega_2 \subset\subset \Omega$ and $\Omega = \Omega_1 \cup \Omega_2 \cup \Gamma$, where $\Gamma = \partial\Omega_1 \cap \partial\Omega_2$ is the interface of Ω_1 and Ω_2 (cf. Fig. 1). For simplicity, we assume that the length/area of Γ satisfies $|\Gamma| = O(1)$. Let \mathcal{M}_h be a triangulation of the domain Ω_1 and \mathcal{M}_H be a triangulation of the domain Ω_2 , and denote Γ_h and Γ_H the two partitions of the interface Γ induced by \mathcal{M}_h and \mathcal{M}_H , respectively. We assume that on the interface Γ , \mathcal{M}_H and \mathcal{M}_h satisfy the matching condition that Γ_h is a refinement of Γ_H . Clearly, each edge/face in Γ_H is composed of some edges/faces in Γ_h . Combining the two triangulations together, we define $\mathcal{M}_{h,H}$ as the triangulation of Ω (See Fig. 1 for an illustration of triangulation). For any element

$K \in \mathcal{M}_h$ (or $K \in \mathcal{M}_H$), we define h_K (or H_K) as $\text{diam}(K)$. Similarly, for each edge/face e of $K_e \in \mathcal{M}_h$ (or E of $K_E \in \mathcal{M}_H$), define h_e as $\text{diam}(e)$ (or H_E as $\text{diam}(E)$). Denote by $h = \max_{K \in \mathcal{M}_h} h_K$ and $H = \max_{K \in \mathcal{M}_H} H_K$. We assume that $h < \epsilon < H$, that $\{\mathcal{M}_H\}$ and $\{\mathcal{M}_h\}$ are shape-regular and quasi-uniform.

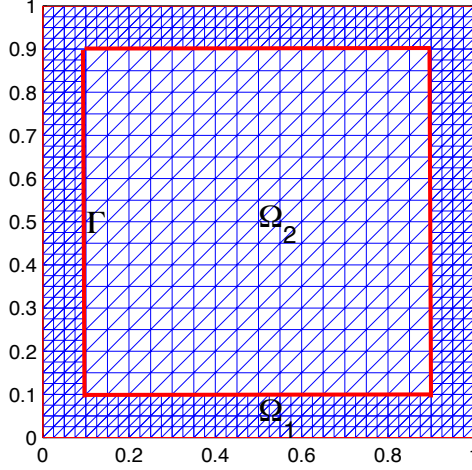


Figure 1: A separation of the domain and a sample mesh.

For any point on Γ , we associate a unit normal \mathbf{n} , which is oriented from Ω_1 to Ω_2 . We also define the jump $[v]$ and average $\{v\}$ of v on the interface Γ as

$$(2.1) \quad [v] := v|_{\Omega_1} - v|_{\Omega_2}, \quad \{v\} := \frac{v|_{\Omega_1} + v|_{\Omega_2}}{2}.$$

Introduce the “energy” space

$$(2.2) \quad V := \{v : v|_{\Omega_i} = v_i, \text{ where } v_i \in H_0^1(\Omega) \cap H^s(\Omega), i = 1, 2\}, \text{ for some } s > \frac{3}{2}.$$

Testing the elliptic problem (1.1) by any $v \in V$, using integration by parts, and using the identity $[vw] = \{v\}[w] + [v]\{w\}$, we obtain

$$\sum_{i=1}^2 \int_{\Omega_i} \mathbf{a}^\epsilon \nabla u_\epsilon \cdot \nabla v - \int_{\Gamma} \{\mathbf{a}^\epsilon \nabla u_\epsilon \cdot \mathbf{n}\} [v] = \int_{\Omega} f v.$$

Define the bilinear form $A_\beta(\cdot, \cdot)$ on $V \times V$:

$$(2.3) \quad A_\beta(u, v) := \sum_{K \in \mathcal{M}_{h,H}} \int_K \mathbf{a}^\epsilon \nabla u \cdot \nabla v$$

$$(2.4) \quad - \sum_{e \in \Gamma_h} \int_e \left(\{ \mathbf{a}^\epsilon \nabla u \cdot \mathbf{n} \} [v] + \beta [u] \{ \mathbf{a}^\epsilon \nabla v \cdot \mathbf{n} \} \right) \\ + J_0(u, v) + J_1(u, v),$$

$$(2.5) \quad J_0(u, v) := \sum_{e \in \Gamma_h} \frac{\gamma_0}{\rho} \int_e [u] [v],$$

$$(2.6) \quad J_1(u, v) := \sum_{e \in \Gamma_h} \gamma_1 \rho \int_e [\mathbf{a}^\epsilon \nabla u \cdot \mathbf{n}] [\mathbf{a}^\epsilon \nabla v \cdot \mathbf{n}],$$

where β is a real number such as $-1, 0, 1$, and $\gamma_0, \gamma_1, \rho > 0$ will be specified later. Define further the linear form $F(\cdot)$ on V :

$$F(v) := \int_\Omega f v.$$

It is easy to check that the solution u_ϵ to the problem (1.1) satisfies the following formulation:

$$(2.7) \quad A_\beta(u_\epsilon, v) = F(v) \quad \forall v \in V.$$

To formulate the FE-MsFEM, we need the oversampling MsFE space on \mathcal{M}_H defined as follows (cf. [15, 42, 26]). For any $K \in \mathcal{M}_H$ with nodes $\{x_i^K\}_{i=1}^{n+1}$, let $\{\varphi_i^K\}_{i=1}^{n+1}$ be the basis of $P_1(K)$ satisfying $\varphi_i^K(x_j^K) = \delta_{ij}, 1 \leq i, j \leq n+1$, where δ_{ij} stands for the Kronecker's symbol. For any $K \in \mathcal{M}_H$, we denote by $S = S(K)$ a macro-element (simplex) which contains K and satisfies that $H_S \leq C_1 H_K$ and $\text{dist}(K, \partial S) \geq C_0 H_K$, where $C_1 > 0$ is independent of H_K and C_0 is from (2.17). We assume that the macro-elements $S(K)$ are also shape-regular. Denote by $\{\varphi_i^S\}_{i=1}^{n+1}$ the nodal basis of $P_1(S)$ such that $\varphi_i^S(x_j^S) = \delta_{ij}, 1 \leq i, j \leq n+1$, where x_j^S are vertices of S .

Let $\psi_i^S \in H^1(S), i = 1, \dots, n+1$, be the solution of the problem

$$(2.8) \quad -\nabla \cdot (\mathbf{a}^\epsilon \nabla \psi_i^S) = 0 \quad \text{in } S, \quad \psi_i^S|_{\partial S} = \varphi_i^S.$$

The oversampling multiscale finite element basis functions over K is defined by

$$(2.9) \quad \bar{\psi}_i^K = c_{ij}^K \psi_j^S|_K \quad \text{in } K,$$

with the constants so chosen that

$$(2.10) \quad \varphi_i^K = c_{ij}^K \varphi_j^S|_K \quad \text{in } K.$$

The existence of the constants c_{ij}^K is guaranteed because $\{\varphi_j^S\}_{j=1}^{n+1}$ also forms a basis of $P_1(K)$.

Let $\text{OMS}(K) = \text{span} \{\bar{\psi}_i^K\}_{i=1}^{n+1}$ be the set of space functions on K . Define the projection $\Pi_K : \text{OMS}(K) \rightarrow P_1(K)$ as

$$\Pi_K \psi = c_i \varphi_i^K \quad \text{if} \quad \psi = c_i \bar{\psi}_i^K \in \text{OMS}(K).$$

Introduce the space of discontinuous piecewise ‘‘OMS’’ functions and the space of discontinuous piecewise linear functions:

$$\begin{aligned} \bar{X}_H &= \{\psi_H : \psi_H|_K \in \text{OMS}(K) \quad \forall K \in \mathcal{M}_H\}, \\ \bar{W}_H &= \{w_H : w_H|_K \in P_1(K) \quad \forall K \in \mathcal{M}_H\}. \end{aligned}$$

Define $\Pi_H : \bar{X}_H \rightarrow \bar{W}_H$ through the relation

$$(2.11) \quad \Pi_H \psi_H|_K = \Pi_K \psi_H \quad \text{for any } K \in \mathcal{M}_H, \psi_H \in \bar{X}_H.$$

The oversampling multiscale finite element space on \mathcal{M}_H is then defined as

$$X_H = \{\psi_H \in \bar{X}_H : \Pi_H \psi_H \in W_H \subset H^1(\Omega_2)\},$$

where $W_H = \bar{W}_H \cap H^1(\Omega_2)$ is the H^1 -conforming linear finite element space over \mathcal{M}_H . In general, $X_H \not\subset H^1(\Omega_2)$ and the requirement $\Pi_H \psi_H \in W_H$ is to impose certain continuity of the functions $\psi_H \in X_H$ across the inter-element boundaries. According to the definition of Π_K , we have $\Pi_K \bar{\psi}_i^K = \varphi_i^K$. Since φ_i^K is continuous across the element, this above requirement $\Pi_H \psi_H \in W_H$ is satisfied naturally since in each node we only have one freedom (unknowns).

Denote by W_h the H^1 -conforming linear finite element space over \mathcal{M}_h and by

$$(2.12) \quad W_h^0 := \{w_h \in W_h : w_h = 0 \text{ on } \partial\Omega_1/\Gamma\}.$$

We define the FE-MsFE approximation space $V_{h,H}$ as

$$(2.13) \quad V_{h,H} := \{v_{h,H} : v_{h,H}|_{\Omega_1} = v_h, v_{h,H}|_{\Omega_2} = v_H, \text{ where } v_h \in W_h^0, v_H \in X_H\}.$$

Note that $V_{h,H} \not\subset V$. We are now ready to define the FE-MsFEM inspired by the formulation (2.7): Find $u_{h,H} \in V_{h,H}$ such that

$$(2.14) \quad A_\beta(u_{h,H}, v_{h,H}) = F(v_{h,H}) \quad \forall v_{h,H} \in V_{h,H}.$$

Remark 2.1. (a) If $\beta = 1$, then the bilinear form A_β is symmetric and, as a consequence, the stiffness matrix is symmetric as well. If $\beta \neq 1$, e.g., $\beta = -1$, then the method is nonsymmetric.

(b) The parameter $\rho > 0$ satisfies that $\rho \leq \epsilon$. In fact, it is chosen as ϵ in our later error analysis, while in practical computation, it may be chosen as the mesh size h .

For further error analysis, we introduce several concepts related to the interface Γ and some discrete norms. Define the set of elements accompanying with the interface partition Γ_h (or Γ_H) as following:

$$(2.15) \quad K_{\Gamma_h} := \{K \in \mathcal{M}_h : K \text{ has an edge/face in } \Gamma_h\},$$

$$(2.16) \quad K_{\Gamma_H} := \{K \in \mathcal{M}_H : K \text{ has an edge/face in } \Gamma_H\}.$$

Clearly, the number of elements in K_{Γ_h} is $O(\frac{1}{h^{n-1}})$ and the number of elements in K_{Γ_H} is $O(\frac{1}{H^{n-1}})$. Moreover, we assume that

$$(2.17) \quad \text{dist}\{\Gamma, \partial\Omega\} \geq C_0 H \geq h + 2\epsilon > 0,$$

where C_0 is a constant. Thus, we can define a narrow subdomain $\Omega_\Gamma \subset \subset \Omega$ surrounding Γ as

$$(2.18) \quad \begin{aligned} \Omega_\Gamma := & \Gamma \cup \{x : x \in \Omega_1, \text{dist}(x, \Gamma) < h + 2\epsilon\} \\ & \cup \{x : x \in \Omega_2, \text{dist}(x, \Gamma) < H + 2\epsilon\}. \end{aligned}$$

Denote by

$$(2.19) \quad \Omega_{\Gamma_H} = \cup\{K : K \in K_{\Gamma_H}\}, \quad \Omega_{\Gamma_h} = \cup\{K : K \in K_{\Gamma_h}\}.$$

It is clear that $\Omega_{\Gamma_H}, \Omega_{\Gamma_h} \subset \Omega_\Gamma$ and $\text{dist}(\Omega_{\Gamma_H}, \partial\Omega_\Gamma), \text{dist}(\Omega_{\Gamma_h}, \partial\Omega_\Gamma) \geq 2\epsilon$, respectively.

Denote by

$$\|v\|_{1,H} = \left(\sum_{K \in \mathcal{M}_H} \|(\mathbf{a}^\epsilon)^{1/2} \nabla v\|_{L^2(K)}^2 \right)^{1/2} \quad \forall v \in \prod_{K \in \mathcal{M}_H} H^1(K).$$

We introduce the following energy norm and the broken norm on the space $V_{h,H}$:

$$(2.20) \quad \|v\|_E := \left(\|v\|_{1,H}^2 + \|(\mathbf{a}^\epsilon)^{1/2} \nabla v\|_{L^2(\Omega_1)}^2 \right)^{1/2},$$

$$(2.21) \quad \begin{aligned} \|v\|_{1,h,H} := & \left(\|v\|_E^2 + \sum_{e \in \Gamma_h} \frac{\gamma_0}{\rho} \| [v] \|_{L^2(e)}^2 + \sum_{e \in \Gamma_h} \gamma_1 \rho \| [\mathbf{a}^\epsilon \nabla v \cdot \mathbf{n}] \|_{L^2(e)}^2 \right. \\ & \left. + \sum_{e \in \Gamma_h} \frac{\rho}{\gamma_0} \| \{ \mathbf{a}^\epsilon \nabla v \cdot \mathbf{n} \} \|_{L^2(e)}^2 \right)^{1/2}. \end{aligned}$$

3 The homogenization results

In this section, we assume that $\mathbf{a}^\epsilon(x)$ has the form $\mathbf{a}(x/\epsilon)$. Moreover, we assume that $a_{ij}(y) \in C_p^1(\mathbb{R}^n)$, where $C_p^1(\mathbb{R}^n)$ stands for the collection of all $C^1(\mathbb{R}^n)$ periodic functions with respect to the unit cube Y . It is shown that under these assumptions (cf. [12, 47]), u_ϵ converges in a suitable topology to the solution of the homogenized equation

$$(3.1) \quad \begin{cases} -\nabla \cdot (\mathbf{a}^* \nabla u_0(x)) = f(x) & \text{in } \Omega, \\ u_0(x) = 0 & \text{on } \partial\Omega, \end{cases}$$

where

$$(3.2) \quad a_{ij}^* = \frac{1}{|Y|} \int_Y a_{ik}(y) \left(\delta_{kj} + \frac{\partial \chi^j}{\partial y_k}(y) \right) dy.$$

Here χ^j is the periodic solution of the cell problem

$$(3.3) \quad -\nabla_y \cdot (\mathbf{a}(y)\nabla_y \chi^j(y)) = \nabla_y \cdot (\mathbf{a}(y)\mathbf{e}_j), \quad j = 1, \dots, n$$

with zero mean, i.e., $\int_Y \chi^j dy = 0$, and \mathbf{e}_j is the unit vector in the j th direction. The variational form of the problem (3.1) is to find $u_0(x) \in H_0^1(\Omega)$ such that

$$(3.4) \quad (\mathbf{a}^* \nabla u_0, \nabla v) = (f, v) \quad \forall v \in H_0^1(\Omega).$$

It can be shown that \mathbf{a}^* is positive definite. Thus by Lax-Milgram lemma, (3.4) has a unique solution. If $f(x) \in L^2(\Omega)$, from the regularity theory of elliptic equations, we have

$$(3.5) \quad \|u_0\|_{H^2(\Omega)} \leq C \|f\|_{L^2(\Omega)}.$$

Let θ_ϵ denote the boundary corrector which is the solution of

$$(3.6) \quad \begin{aligned} -\nabla \cdot (\mathbf{a}^\epsilon \nabla \theta_\epsilon) &= 0 && \text{in } \Omega, \\ \theta_\epsilon &= -\chi^j(x/\epsilon) \frac{\partial u_0(x)}{\partial x_j} && \text{on } \partial\Omega. \end{aligned}$$

From the Maximum Principle, we have

$$(3.7) \quad \|\theta_\epsilon\|_{L^\infty(\Omega)} \lesssim |u_0|_{W^{1,\infty}(\Omega)}.$$

In the following part, for convenience's sake, we will set

$$(3.8) \quad u_1(x, x/\epsilon) = u_0(x) + \epsilon \chi^j(x/\epsilon) \frac{\partial u_0(x)}{\partial x_j}.$$

The following error estimates are known (cf. e.g. [14, 49, 16]).

Theorem 3.1. *Assume that $u_0 \in H^2(\Omega) \cap W^{1,\infty}(\Omega)$. Then there exists a constant C independent of ϵ , the domain Ω , and the function f such that*

$$(3.9) \quad \|\nabla(u_\epsilon - u_1 - \epsilon\theta_\epsilon)\|_{L^2(\Omega)} \leq C\epsilon |u_0|_{H^2(\Omega)}.$$

Moreover, the boundary corrector θ_ϵ satisfies the estimate

$$(3.10) \quad \|\epsilon \nabla \theta_\epsilon\|_{L^2(\Omega)} \leq C\epsilon |u_0|_{H^2(\Omega)} + C\sqrt{\epsilon |\partial\Omega|} |u_0|_{W^{1,\infty}(\Omega)}.$$

where $|\partial\Omega|$ stands for the measure of the boundary $\partial\Omega$.

The following regularity estimate is an analogy of the classical interior estimate for elliptic equations in [40, Theorem 8.8, P.183].

Lemma 3.2. *Let $w \in H^1(D)$ be the weak solution of the equation*

$$-\nabla \cdot (\mathbf{a}^\epsilon(x)\nabla w) = g(x), \quad x \in D,$$

where $\mathbf{a}^\epsilon(x)$ satisfies (1.2) and $g \in L^2(D)$. Then for any subdomain $D' \subset\subset D$, we have $w \in H^2(D')$ and

$$(3.11) \quad |w|_{H^2(D')} \lesssim \left(\frac{1}{d'} + \frac{1}{r} \right) |w|_{H^1(D)} + \|g\|_{L^2(D)}$$

where $d' = \text{dist}(D', \partial D)$ and r is a constant such that $|\mathbf{a}^\epsilon(x) - \mathbf{a}^\epsilon(y)| \leq r|x - y|$.

Remark 3.1. The H^2 norm interior estimate for elliptic equations is well-known in the literature. The importance in above estimate is the explicit dependence of the bound on d' and r which is crucial in our analysis.

Proof. First, we define the difference quotient as follow:

$$\Delta^h v(x) = \Delta_k^h v = \frac{v(x + he_k) - v(x)}{h},$$

where $e_k, 1 \leq k \leq n$ is the unit coordinate vector in the x_k direction. And then, following the proof presented in [40, Theorem 8.8, P.183], we obtain

$$\begin{aligned} & \lambda \int_D |\xi \nabla(\Delta^h w)|^2 dx \\ & \leq \left(\frac{1}{r} \|\nabla w\|_{L^2(D)} + \|g\|_{L^2(D)} \right) \left(\|\xi \nabla(\Delta^h w)\|_{L^2(D)} + 2 \|\Delta^h w \nabla \xi\|_{L^2(D)} \right) \\ & \quad + C \|\xi \nabla(\Delta^h w)\|_{L^2(D)} \|\Delta^h w \nabla \xi\|_{L^2(D)}, \end{aligned}$$

where $\xi \in C_0^1(D)$ is the cut-off function such that $0 \leq \xi \leq 1$, $\xi = 1$ in D' , and $|\nabla \xi| \leq 2/d'$ in D . By use of the Young's inequality and the Lemma 7.23 in [40, P.168], it follows that

$$\begin{aligned} \|\xi \Delta^h(\nabla w)\|_{L^2(D)} & \leq C \left(\frac{1}{r} \|\nabla w\|_{L^2(D)} + \|g\|_{L^2(D)} + \|\Delta^h w \nabla \xi\|_{L^2(D)} \right) \\ & \leq C \left(\frac{1}{r} + \frac{1}{d'} \right) \|\nabla w\|_{L^2(D)} + C \|g\|_{L^2(D)}. \end{aligned}$$

By the Lemma 7.24 in [40, P.169] we obtain $\nabla w \in H^1(D')$, so that $w \in H^2(D')$ and the estimate (3.11) holds. This completes the proof. \square

Utilizing the above H^2 interior estimate to equation $-\nabla \cdot (\mathbf{a}^* \nabla u_{0x_j}) = f_{x_j}, j = 1, \dots, n$, where x_j is the coordinate variable in the j th direction, we obtain

Lemma 3.3. Let u_0 be the solution to (3.4). Assume that $u_0 \in H^2(D)$ and $f \in H^1(D)$. Then for any subdomain $D' \subset\subset D$ with $d' = \text{dist}(D', \partial D)$, we have

$$(3.12) \quad |u_0|_{H^3(D')} \lesssim \frac{1}{d'} |u_0|_{H^2(D)} + \|\nabla f\|_{L^2(D)}.$$

Further, by use of the H^2 interior estimate (3.11), we obtain an H^2 semi-norm interior estimate of the error $u_\epsilon - u_1$ in the narrow domain Ω_Γ .

Theorem 3.4. *Assume that $u_0 \in H^2(\Omega) \cap W^{1,\infty}(\Omega)$, and $f|_{\Omega_\Gamma} \in H^1(\Omega_\Gamma)$. Then for any subdomain $\Omega' \subset\subset \Omega_\Gamma$ with $\text{dist}(\Omega', \partial\Omega_\Gamma) \geq 2\epsilon$, we have*

$$(3.13) \quad |u_\epsilon - u_1|_{H^2(\Omega')} \lesssim |u_0|_{H^2(\Omega)} + \epsilon \|\nabla f\|_{L^2(\Omega_\Gamma)} + \frac{1}{\sqrt{\epsilon}} |u_0|_{W^{1,\infty}(\Omega)}.$$

Proof. It is shown that, for any $\varphi \in H_0^1(\Omega)$ (see [14, p.550] or [15, p.125]),

$$(3.14) \quad \begin{aligned} & (\mathbf{a}(x/\epsilon)\nabla(u_\epsilon - u_1), \nabla\varphi)_\Omega \\ &= (\mathbf{a}^*\nabla u_0, \nabla\varphi)_\Omega - \left(\mathbf{a}(x/\epsilon)\nabla \left(u_0 + \epsilon\chi^k \frac{\partial u_0}{\partial x_k} \right), \nabla\varphi \right)_\Omega \\ &= \epsilon \int_\Omega a_{ij}(x/\epsilon)\chi^k \frac{\partial^2 u_0}{\partial x_j \partial x_k} \frac{\partial \varphi}{\partial x_i} - \epsilon \int_\Omega \alpha_{ij}^k(x/\epsilon) \frac{\partial^2 u_0}{\partial x_j \partial x_k} \frac{\partial \varphi}{\partial x_i}, \end{aligned}$$

where $\alpha_{ij}^k(y) \in H_{loc}^1(\mathbb{R}^n)$ are Y -periodic and dependent only on the coefficients $\mathbf{a}(y)$ (see [47, p.6]). According to the assumption, there exists a subdomain $\Omega_c \subset\subset \Omega_\Gamma$ such that $\Omega' \subset\subset \Omega_c$ with $d_0 = \text{dist}(\Omega', \partial\Omega_c) \geq \epsilon$ and $d_1 = \text{dist}(\Omega_c, \partial\Omega_\Gamma) \geq \epsilon$. From (3.14), it follows that in Ω_c ,

$$\nabla \cdot (\mathbf{a}(x/\epsilon)\nabla(u_\epsilon - u_1)) = \epsilon \frac{\partial}{\partial x_i} \left(a_{ij}(x/\epsilon)\chi^k \frac{\partial^2 u_0}{\partial x_j \partial x_k} - \alpha_{ij}^k(x/\epsilon) \frac{\partial^2 u_0}{\partial x_j \partial x_k} \right).$$

Thus, from Lemma 3.2, it follows that

$$|u_\epsilon - u_1|_{H^2(\Omega')} \lesssim \left(\frac{1}{d_0} + \frac{1}{\epsilon} \right) |u_\epsilon - u_1|_{H^1(\Omega_c)} + |u_0|_{H^2(\Omega_c)} + \epsilon |u_0|_{H^3(\Omega_c)}.$$

Hence, from Theorem 3.1 and Lemma 3.3, it follows the result (3.13) immediately. \square

We conclude this section with a local H^2 semi-norm estimate for u_1 in Ω_{Γ_h} , which will be used in the convergence analysis.

Lemma 3.5. *Assume that $u_0 \in H^2(\Omega) \cap W^{1,\infty}(\Omega)$, and $f|_{\Omega_\Gamma} \in H^1(\Omega_\Gamma)$. Then,*

$$(3.15) \quad |u_1|_{H^2(\Omega_{\Gamma_h})} \lesssim |u_0|_{H^2(\Omega_\Gamma)} + \epsilon^{-1} h^{1/2} |u_0|_{W^{1,\infty}(\Omega_{\Gamma_h})} + \epsilon \|\nabla f\|_{L^2(\Omega_\Gamma)},$$

where Ω_{Γ_h} and Ω_Γ are defined in (2.19) and (2.18), respectively.

Proof. It is easy to see that

$$\begin{aligned} |u_1|_{H^2(\Omega_{\Gamma_h})} &\leq |u_0|_{H^2(\Omega_{\Gamma_h})} + \left| \epsilon\chi^j \frac{\partial u_0}{\partial x_j} \right|_{H^2(\Omega_{\Gamma_h})} \\ &\lesssim |u_0|_{H^2(\Omega_{\Gamma_h})} + \epsilon^{-1} \left| \frac{\partial u_0}{\partial x_j} \right|_{L^2(\Omega_{\Gamma_h})} + \epsilon |u_0|_{H^3(\Omega_{\Gamma_h})}. \end{aligned}$$

Thus, from Lemma 3.3, it follows that

$$|u_1|_{H^2(\Omega_{\Gamma_h})} \lesssim |u_0|_{H^2(\Omega_\Gamma)} + \epsilon \|\nabla f\|_{L^2(\Omega_\Gamma)} + \epsilon^{-1} |\Omega_{\Gamma_h}|^{1/2} \|\nabla u_0\|_{L^\infty(\Omega_{\Gamma_h})},$$

which, combining with the fact that $|\Omega_{\Gamma_h}| = O(h)$, yields the result (3.15). \square

4 Approximation properties of the FE-MsFE space $V_{h,H}$

In this section, we give some approximation properties for the oversampling MsFE space X_H and the linear FE space W_h , respectively.

4.1 Approximation properties of oversampling MsFE space X_H

We first recall a stability estimate for Π_H (see [15, Lemma 9.8] or [28, Appendix B]).

Lemma 4.1. *There exist constants γ and C independent of H and ϵ such that if $H_K \leq \gamma$ and $\epsilon/H_K \leq \gamma$ for all $K \in \mathcal{M}_H$, the following estimates are valid*

$$C^{-1} \|\nabla \Pi_H w_H\|_{L^2(K)} \leq \|\nabla w_H\|_{L^2(K)} \leq C \|\nabla \Pi_H w_H\|_{L^2(K)} \quad \forall w_H \in X_H.$$

Next, we give some approximation properties of the oversampling MsFE space $\text{OMS}(K)$.

Lemma 4.2. *For any $K \in \mathcal{M}_H$, there exists $\phi_H \in \text{OMS}(K)$ such that the following estimates hold:*

$$(4.1) \quad |u_1 - \phi_H|_{H^1(K)} \lesssim H_K |u_0|_{H^2(K)} + \epsilon H_K^{n/2-1} |u_0|_{W^{1,\infty}(K)},$$

$$(4.2) \quad \|u_1 - \phi_H\|_{L^2(K)} \lesssim H_K^2 |u_0|_{H^2(K)} + \epsilon H_K^{n/2} |u_0|_{W^{1,\infty}(K)},$$

$$(4.3) \quad |u_1 - \phi_H|_{H^2(K)} \lesssim \epsilon^{-1} H_K |u_0|_{H^2(K)} + H_K^{n/2-1} |u_0|_{W^{1,\infty}(K)} + \epsilon |u_0|_{H^3(K)}.$$

Proof. We take

$$(4.4) \quad \phi_H = \sum_{x_i^K \text{ node of } K} u_0(x_i^K) \bar{\psi}_i(x),$$

then

$$\Pi_K \phi_H = I_H u_0,$$

where $I_H : C(\bar{\Omega}_2) \rightarrow W_H$ is the standard Lagrange interpolation operator over linear finite element space. By the asymptotic expansion, we know that

$$(4.5) \quad \phi_H = I_H u_0 + \epsilon \chi^j \frac{\partial(I_H u_0)}{\partial x_j} + \epsilon \theta_\epsilon^S,$$

where $\theta_\epsilon^S \in H^1(S)$ is the boundary corrector given by

$$(4.6) \quad -\nabla \cdot (\mathbf{a}^\epsilon \nabla \theta_\epsilon^S) = 0 \quad \text{in } S, \quad \theta_\epsilon^S|_{\partial S} = -\chi^j \frac{\partial(I_H u_0)}{\partial x_j}.$$

By the Maximum Principle we have

$$(4.7) \quad \|\theta_\epsilon^S\|_{L^\infty(S)} \lesssim |I_H u_0|_{W^{1,\infty}(S)} \lesssim |u_0|_{W^{1,\infty}(K)},$$

which together with the interior estimate in Avellaneda and Lin [7, Lemma 16] imply that

$$(4.8) \quad \|\nabla \theta_\epsilon^S\|_{L^\infty(K)} \lesssim H_K^{-1} \|\theta_\epsilon^S\|_{L^\infty(S)} \lesssim H_K^{-1} |u_0|_{W^{1,\infty}(K)}.$$

Therefore

$$(4.9) \quad \left\| \nabla \left(\phi_H - I_H u_0 - \epsilon \chi^j \frac{\partial(I_H u_0)}{\partial x_j} \right) \right\|_{L^2(K)} \lesssim \epsilon H_K^{-1} |u_0|_{W^{1,\infty}(K)} |K|^{1/2} \\ \lesssim \epsilon H_K^{n/2-1} |u_0|_{W^{1,\infty}(K)}.$$

Further, since

$$\|\nabla(u_0 - I_H u_0)\|_{L^2(K)} \lesssim H_K |u_0|_{H^2(K)}, \\ \left\| \epsilon \nabla \left(\chi^j \frac{\partial(u_0 - I_H u_0)}{\partial x_j} \right) \right\|_{L^2(K)} \lesssim (H_K + \epsilon) |u_0|_{H^2(K)},$$

we obtain the result (4.1) immediately.

To prove the estimate (4.2), we first notice that, from (4.7),

$$\|\theta_\epsilon^S\|_{L^2(K)} \leq |K|^{1/2} \|\theta_\epsilon^S\|_{L^\infty(K)} \lesssim H_K^{n/2} |u_0|_{W^{1,\infty}(K)}.$$

Therefore

$$(4.10) \quad \left\| \phi_H - \left(I_H u_0 + \epsilon \chi^j \frac{\partial(I_H u_0)}{\partial x_j} \right) \right\|_{L^2(K)} \lesssim \epsilon H_K^{n/2} |u_0|_{W^{1,\infty}(K)}.$$

Further, since

$$\|u_0 - I_H u_0\|_{L^2(K)} \lesssim H_K^2 |u_0|_{H^2(K)}, \\ \left\| \epsilon \chi^j \frac{\partial(u_0 - I_H u_0)}{\partial x_j} \right\|_{L^2(K)} \lesssim \epsilon H_K |u_0|_{H^2(K)},$$

we obtain the result (4.2) immediately.

To prove the estimate (4.3), it is easy to see that

$$(4.11) \quad |u_0 - I_H u_0|_{H^2(K)} \lesssim |u_0|_{H^2(K)},$$

$$(4.12) \quad \left| \epsilon \chi^j \frac{\partial(u_0 - I_H u_0)}{\partial x_j} \right|_{H^2(K)} \lesssim (1 + \epsilon^{-1} H_K) |u_0|_{H^2(K)} + \epsilon |u_0|_{H^3(K)}.$$

Let D be a simplex such that

$$K \subset\subset D \subset\subset S \text{ and } \text{dist}(K, \partial D), \text{dist}(D, \partial S) \gtrsim H_K.$$

From Lemma 3.2 and following the proof of (4.8), we have

$$|\theta_\epsilon^S|_{H^2(K)} \lesssim (H_K^{-1} + \epsilon^{-1}) |\theta_\epsilon^S|_{H^1(D)} \lesssim H_K^{n/2-1} (H_K^{-1} + \epsilon^{-1}) \|\nabla u_0\|_{L^\infty(K)},$$

which, combining with (4.11) and (4.12), yields the result immediately. This completes the proof. \square

From Lemma 4.2, we have the following local approximation estimates in K_{Γ_H} .

Lemma 4.3. *There exists $\psi_H \in X_H$ such that,*

$$(4.13) \quad \left(\sum_{K \in K_{\Gamma_H}} \|u_1 - \psi_H\|_{L^2(K)}^2 \right)^{1/2} \lesssim H^2 |u_0|_{H^2(\Omega_{\Gamma_H})} + \epsilon \sqrt{H} |u_0|_{W^{1,\infty}(\Omega_{\Gamma_H})},$$

$$(4.14) \quad \left(\sum_{K \in K_{\Gamma_H}} |u_1 - \psi_H|_{H^1(K)}^2 \right)^{1/2} \lesssim H |u_0|_{H^2(\Omega_{\Gamma_H})} + \frac{\epsilon}{\sqrt{H}} |u_0|_{W^{1,\infty}(\Omega_{\Gamma_H})}$$

$$(4.15) \quad \left(\sum_{K \in K_{\Gamma_H}} |u_1 - \psi_H|_{H^2(K)}^2 \right)^{1/2} \lesssim \frac{H}{\epsilon} |u_0|_{H^2(\Omega_{\Gamma})} + \epsilon \|\nabla f\|_{L^2(\Omega_{\Gamma})} + \frac{1}{\sqrt{H}} |u_0|_{W^{1,\infty}(\Omega_{\Gamma_H})},$$

where Ω_{Γ_H} is defined in (2.19).

Proof. We take

$$(4.16) \quad \psi_H = \sum_{p_j \text{ node of } \mathcal{M}_H} u_0(p_j) \bar{\psi}_j(x) \in X_H,$$

then $\psi_H|_K = \phi_H$, which is defined in Lemma 4.2. From (4.2), it follows that

$$\begin{aligned} \sum_{K \in K_{\Gamma_H}} \|u_1 - \psi_H\|_{L^2(K)}^2 &\lesssim H^4 |u_0|_{H^2(\Omega_{\Gamma_H})}^2 + \epsilon^2 H^n |u_0|_{W^{1,\infty}(\Omega_{\Gamma_H})}^2 \sum_{K \in K_{\Gamma_H}} 1 \\ &\lesssim H^4 |u_0|_{H^2(\Omega_{\Gamma_H})}^2 + \epsilon^2 H |u_0|_{W^{1,\infty}(\Omega_{\Gamma_H})}^2, \end{aligned}$$

which yields (4.13) immediately. Note here we have used the fact that the number of elements in K_{Γ_H} is $O(\frac{|\Gamma|}{H^{n-1}})$. Similarly, (4.14) follows from (4.1).

It remains to prove (4.15). From (4.3) and Lemma 3.3, it follows that

$$\begin{aligned} \sum_{K \in K_{\Gamma_H}} |u_1 - \psi_H|_{H^2(K)}^2 &\lesssim \epsilon^{-2} H^2 |u_0|_{H^2(\Omega_{\Gamma_H})}^2 + \epsilon^2 |u_0|_{H^3(\Omega_{\Gamma_H})}^2 \\ &\quad + H^{n-2} |u_0|_{W^{1,\infty}(\Omega_{\Gamma_H})}^2 \sum_{K \in K_{\Gamma_H}} 1 \\ &\lesssim (\epsilon^{-2} H^2 + 1) |u_0|_{H^2(\Omega_{\Gamma})}^2 + \epsilon^2 \|\nabla f\|_{L^2(\Omega_{\Gamma})}^2 + H^{-1} |u_0|_{W^{1,\infty}(\Omega_{\Gamma_H})}^2, \end{aligned}$$

which yields (4.15) immediately. The proof is completed. \square

From Lemma 4.2, Theorem 3.1, via taking the same ψ_H in Lemma 4.3, we also have the following result which gives an approximation estimate of the space X_H (cf. [28, 26, 15]).

Lemma 4.4. *There exists $\psi_H \in X_H$ such that,*

$$(4.17) \quad \|u_\epsilon - \psi_H\|_{1,H} \lesssim H |u_0|_{H^2(\Omega)} + \frac{\epsilon}{H} |u_0|_{W^{1,\infty}(\Omega_2)} + \sqrt{\epsilon} |u_0|_{W^{1,\infty}(\Omega)}.$$

4.2 Approximation properties of linear FE space W_h

Since $|\Omega_1|$, the area/volume of Ω_1 , may be small, we prefer estimates with explicit dependence on it. To attain this aim, we use the Scott-Zhang interpolation instead of the standard FE interpolation in this subsection.

We first introduce the Scott-Zhang interpolation operator $Z_h : H_E^1(\Omega_1) \rightarrow W_h^0$, where $H_E^1(\Omega_1) := \{v \in H^1(\Omega_1) : v = 0 \text{ on } \partial\Omega_1 \setminus \Gamma\}$. For any node z in \mathcal{M}_h , let $\phi_z(x)$ be the nodal basis function associated with z and let e_z be an edge/face with one vertex at z , then the Scott-Zhang interpolation operator is defined as [55]:

$$(4.18) \quad Z_h v = \sum_{\text{node } z \text{ in } \mathcal{M}_h} \left(\int_{e_z} \psi_z v \right) \phi_z \quad \forall v \in H_E^1(\Omega_1),$$

where $\psi_z(x)$ is a linear function that satisfies $\int_{e_z} \psi_z(x) w(x) = w(z)$ for any linear function $w(x)$ on e_z . Suppose $e_z \subset \partial\Omega_1$ for $z \in \partial\Omega_1$. It is easy to check that $\|\psi_z\|_{L^\infty(\Omega_z)} \lesssim h_{e_z}^{-(n-1)}$, $\|\nabla \psi_z\|_{L^\infty(\Omega_z)} \lesssim h_{e_z}^{-n}$, where $\Omega_z := \text{supp}(\phi_z)$, and

$$(4.19) \quad Z_h v = v \quad \forall v \in W_h^0.$$

This operator enjoys the following stability and interpolation estimates (see [55]):

Lemma 4.5. *For any $K \in \mathcal{M}_h$, we have*

$$(4.20) \quad \|Z_h v\|_{L^\infty(K)} \lesssim \|v\|_{L^\infty(\tilde{K})}, \quad \|\nabla Z_h v\|_{L^\infty(K)} \lesssim \|\nabla v\|_{L^\infty(\tilde{K})},$$

$$(4.21) \quad \|v - Z_h v\|_{L^2(K)} + h_K \|v - Z_h v\|_{H^1(K)} \lesssim h_K^2 |v|_{H^2(\tilde{K})},$$

$$(4.22) \quad \|v - Z_h v\|_{L^\infty(K)} \lesssim h_K^2 |v|_{W^{2,\infty}(\tilde{K})},$$

where \tilde{K} is the union of all elements in \mathcal{M}_h having nonempty intersection with K .

Moreover, we need the following error estimate between u_1 and its Scott-Zhang interpolant which uses only the regularity of the homogenization solution u_0 .

Lemma 4.6. *For any $K \in \mathcal{M}_h$, we have*

$$(4.23) \quad |u_1 - Z_h u_1|_{H^1(K)} \lesssim \left(h_K + \epsilon + \frac{h_K^2}{\epsilon} \right) |u_0|_{H^2(\tilde{K})} + \frac{h_K^{n/2+1}}{\epsilon} |u_0|_{W^{1,\infty}(K)},$$

where \tilde{K} is defined in Lemma 4.5.

Proof. Denote by $v_j := \frac{\partial u_0}{\partial x_j}$. It is easy to see that

$$\begin{aligned} |u_1 - Z_h u_1|_{H^1(K)} &\lesssim |u_0 - Z_h u_0|_{H^1(K)} + \epsilon |\chi^j v_j - Z_h(\chi^j v_j)|_{H^1(K)} \\ &\lesssim |u_0 - Z_h u_0|_{H^1(K)} + \epsilon |(\chi^j - Z_h \chi^j) v_j|_{H^1(K)} \\ &\quad + \epsilon |Z_h \chi^j (v_j - \langle v_j \rangle_K)|_{H^1(K)} + \epsilon |Z_h \chi^j \langle v_j \rangle_K - Z_h(\chi^j v_j)|_{H^1(K)} \\ &:= \text{I} + \text{II} + \text{III} + \text{IV}. \end{aligned}$$

where $\langle \cdot \rangle_K = \frac{1}{|K|} \int_K (\cdot) dx$. From (4.21), we have

$$(4.24) \quad \text{I} \lesssim h_K |u_0|_{H^2(\tilde{K})}.$$

From the facts that $|\nabla \chi^j| \lesssim \epsilon^{-1}$, $|\nabla^2 \chi^j| \lesssim \epsilon^{-2}$ and (4.20)–(4.22), we have

$$(4.25) \quad \text{II} \lesssim \frac{h_K^{n/2+1}}{\epsilon} |u_0|_{W^{1,\infty}(K)} + \frac{h_K^2}{\epsilon} |u_0|_{H^2(K)},$$

$$(4.26) \quad \text{III} \lesssim (h_K + \epsilon) |u_0|_{H^2(K)},$$

where we have used the Poincaré inequality to derive the second inequality. It remains to estimate IV. According to the definition of Scott-Zhang interpolation, we have

$$\begin{aligned} \text{IV} &= \epsilon \left| \sum_{\text{node } z \in K} \phi_z(x) \int_{e_z} \psi_z \chi^j (\langle v_j \rangle_K - v_j) \right|_{H^1(K)} \\ &\lesssim \epsilon h_K^{n/2} \left| \sum_{\text{node } z \in K} \nabla \phi_z(x) \int_{e_z} \psi_z \chi^j (\langle v_j \rangle_K - v_j) \right| \\ &\lesssim \epsilon h_K^{-n/2} \sum_{\text{node } z \in K} \sum_{j=1}^n \int_{e_z} |\langle v_j \rangle_K - v_j|. \end{aligned}$$

For each node $z \in K$, there exist a number $M_z \lesssim 1$ and a sequence of elements $K_{z,m} \subset \tilde{K}$, $m = 1, \dots, M_z$, such that $K_{z,1} = K$, $K_{z,i}$ and $K_{z,i+1}$ have a common edge/face $e_{z,i}$, $i = 1, \dots, M_z - 1$, and $e_{z,M_z} := e_z$ is an edge/face of K_{z,M_z} . Clearly, we have

$$\begin{aligned} \int_{e_z} |\langle v_j \rangle_K - v_j| &\leq \int_{e_{z,M_z}} |\langle v_j \rangle_{K_{z,M_z}} - v_j| + h_{e_{z,M_z}} |\langle v_j \rangle_{K_{z,1}} - \langle v_j \rangle_{K_{z,M_z}}| \\ &\leq \int_{e_{z,M_z}} |\langle v_j \rangle_{K_{z,M_z}} - v_j| \\ &\quad + h_{e_{z,M_z}} \left| \langle v_j \rangle_{K_{z,1}} - \frac{1}{h_{z,1}} \int_{e_{z,1}} v_j + \frac{1}{h_{z,1}} \int_{e_{z,1}} (v_j - \langle v_j \rangle_{K_{z,2}}) \right. \\ &\quad \left. + \dots + \frac{1}{h_{z,M_z-1}} \int_{e_{z,M_z-1}} (v_j - \langle v_j \rangle_{K_{z,M_z}}) \right| \\ &\lesssim \sum_{m=1}^{M_z} \int_{\partial K_{z,m}} |\langle v_j \rangle_{K_{z,m}} - v_j| \\ &\lesssim h_K^{(n-1)/2} \sum_{m=1}^{M_z} \left\| \langle v_j \rangle_{K_{z,m}} - v_j \right\|_{L^2(\partial K_{z,m})}. \end{aligned}$$

Thus, by the trace inequality and Poincaré inequality, we obtain

$$\begin{aligned} \text{IV} &\lesssim \epsilon h_K^{-1/2} \sum_{\text{node } z \in K} \sum_{j=1}^n \sum_{m=1}^{M_z} \left(h_K^{-1/2} \left\| \langle v_j \rangle_{K_{z,m}} - v_j \right\|_{L^2(K_{z,m})} \right. \\ &\quad \left. + h_K^{1/2} \left\| \nabla (\langle v_j \rangle_{K_{z,m}} - v_j) \right\|_{L^2(K_{z,m})} \right) \\ &\lesssim \epsilon \sum_{j=1}^n \|\nabla v_j\|_{L^2(\bar{K})} \lesssim \epsilon |u_0|_{H^2(\bar{K})}, \end{aligned}$$

which, combining with (4.24)–(4.26), yields the result immediately. \square

From Lemma 4.6 and Theorem 3.1, we have the following result which gives H^1 approximation estimates of the space W_h . The proof is omitted.

Lemma 4.7. *Let $\hat{u}_h := Z_h u_1$. Then*

$$(4.27) \quad |u_1 - \hat{u}_h|_{H^1(\Omega_1)} \lesssim \epsilon |u_0|_{H^2(\Omega_1)} + \frac{h}{\epsilon} |\Omega_1|^{1/2} |u_0|_{W^{1,\infty}(\Omega_1)},$$

$$(4.28) \quad |u_1 - \hat{u}_h|_{H^1(\Omega_{\Gamma_h})} \lesssim \epsilon |u_0|_{H^2(\Omega_1)} + \frac{h^{3/2}}{\epsilon} |u_0|_{W^{1,\infty}(\Omega_{\Gamma_h})},$$

where Ω_{Γ_h} is defined in (2.19).

5 Error estimates for the FE-MsFEM

In this section we derive the H^1 -error estimate for the FE-MsFEM in the case where $\beta = 1$. For other cases such that $\beta = 0, -1$, the analysis is similar and is omitted here. Since the convergence analysis is only done for the periodic coefficient case, we will fix $\rho = \epsilon$ in the later analysis.

The following Lemma gives an inverse estimate for the function in space $\text{OMS}(K)$.

Lemma 5.1. *Assume that $v_H \in \text{OMS}(K)$. Then, we have*

$$(5.1) \quad |v_H|_{H^2(K)} \lesssim (\epsilon^{-1} + H^{-1}) |v_H|_{H^1(K)}.$$

Proof. Assume that $v_H = c_i \bar{\psi}_i^K$. By the definition of $\bar{\psi}_i^K$, we can extend the v_H to the macro element $S \supset K$ as following: $v_H = c_i c_{ij}^K \psi_j^S$, and $\Pi_K v_H = c_i c_{ij}^K \varphi_j^S$, where c_{ij}^K, ψ_j^S , and φ_j^S are defined in Section 2 (see (2.8)–(2.10)). It is easy to verify that v_H satisfies

$$\begin{cases} -\nabla \cdot (\mathbf{a}^\epsilon(x) \nabla v_H(x)) = 0, & x \in S, \\ v_H = \Pi_K v_H, & x \in \partial S. \end{cases}$$

Hence, from Lemma 3.2 and $\text{dist}(K, \partial S) \gtrsim H_K$, it follows that

$$|v_H|_{H^2(K)} \lesssim (\epsilon^{-1} + H^{-1}) \|\nabla v_H\|_{L^2(S)},$$

which yields

$$|v_H|_{H^2(K)} \lesssim (\epsilon^{-1} + H^{-1}) \|\nabla \Pi_K v_H\|_{L^2(S)} \lesssim (\epsilon^{-1} + H^{-1}) \|\nabla \Pi_K v_H\|_{L^2(K)}.$$

Therefore, from Lemma 4.1, it follows the result (5.1) immediately. \square

The following lemma gives the continuity and coercivity of the bilinear form $A_\beta(\cdot, \cdot)$ for the FE-MsFEM.

Lemma 5.2. *We have*

$$(5.2) \quad |A_\beta(v, w)| \leq 2 \|v\|_{1,h,H} \|w\|_{1,h,H} \quad \forall v, w \in V_{h,H}.$$

For any $0 < \gamma_1 \lesssim 1$, there exists a constant α_0 independent of h, H, ϵ , and the penalty parameters such that, if $\gamma_0 \geq \alpha_0/\gamma_1$, then

$$(5.3) \quad A_\beta(v_{h,H}, v_{h,H}) \geq \frac{1}{2} \|v_{h,H}\|_{1,h,H}^2 \quad \forall v_{h,H} \in V_{h,H}.$$

Proof. (5.2) is a direct consequence of the definitions (2.3)–(2.6), (2.20), (2.21), and the Cauchy-Schwarz inequality.

It remains to prove (5.3). We have,

$$\begin{aligned} A_\beta(v_{h,H}, v_{h,H}) &= \sum_{K \in \mathcal{M}_{h,H}} \|(\mathbf{a}^\epsilon)^{1/2} \nabla v_{h,H}\|_{L^2(K)}^2 - 2 \sum_{e \in \Gamma_h} \int_e \{\mathbf{a}^\epsilon \nabla v_{h,H} \cdot \mathbf{n}\} [v_{h,H}] \\ &\quad + \sum_{e \in \Gamma_h} \left(\frac{\gamma_0}{\epsilon} \| [v_{h,H}] \|_{L^2(e)}^2 + \gamma_1 \epsilon \| \{\mathbf{a}^\epsilon \nabla v_{h,H} \cdot \mathbf{n}\} \|_{L^2(e)}^2 \right) \\ &= \|v_{h,H}\|_{1,h,H}^2 - \sum_{e \in \Gamma_h} \frac{\epsilon}{\gamma_0} \| \{\mathbf{a}^\epsilon \nabla v_{h,H} \cdot \mathbf{n}\} \|_{L^2(e)}^2 - 2 \sum_{e \in \Gamma_h} \int_e \{\mathbf{a}^\epsilon \nabla v_{h,H} \cdot \mathbf{n}\} [v_{h,H}]. \end{aligned}$$

It is obvious that,

$$\begin{aligned} 2 \sum_{e \in \Gamma_h} \int_e \{\mathbf{a}^\epsilon \nabla v_{h,H} \cdot \mathbf{n}\} [v_{h,H}] &\leq 2 \sum_{e \in \Gamma_h} \| \{\mathbf{a}^\epsilon \nabla v_{h,H} \cdot \mathbf{n}\} \|_{L^2(e)} \| [v_{h,H}] \|_{L^2(e)} \\ &\leq \sum_{e \in \Gamma_h} \frac{\gamma_0}{2\epsilon} \| [v_{h,H}] \|_{L^2(e)}^2 + \sum_{e \in \Gamma_h} \frac{2\epsilon}{\gamma_0} \| \{\mathbf{a}^\epsilon \nabla v_{h,H} \cdot \mathbf{n}\} \|_{L^2(e)}^2. \end{aligned}$$

Therefore,

$$A_\beta(v_{h,H}, v_{h,H}) \geq \|v_{h,H}\|_{1,h,H}^2 - \sum_{e \in \Gamma_h} \frac{\gamma_0}{2\epsilon} \| [v_{h,H}] \|_{L^2(e)}^2 - \sum_{e \in \Gamma_h} \frac{3\epsilon}{\gamma_0} \| \{\mathbf{a}^\epsilon \nabla v_{h,H} \cdot \mathbf{n}\} \|_{L^2(e)}^2.$$

It is clear that, for any $e \in \Gamma_h$,

$$\{\mathbf{a}^\epsilon \nabla v_{h,H} \cdot \mathbf{n}\} \Big|_e = (\mathbf{a}^\epsilon \nabla v_H) \cdot \mathbf{n} + \frac{1}{2} [\mathbf{a}^\epsilon \nabla v_{h,H} \cdot \mathbf{n}] \Big|_e.$$

We have

$$(5.4) \quad \begin{aligned} A_\beta(v_{h,H}, v_{h,H}) &\geq \|v_{h,H}\|_{1,h,H}^2 - \sum_{e \in \Gamma_h} \frac{\gamma_0}{2\epsilon} \| [v_{h,H}] \|_{L^2(e)}^2 \\ &\quad - \frac{6\epsilon}{\gamma_0} \sum_{e \in \Gamma_h} \left(\|(\mathbf{a}^\epsilon \nabla v_H) \cdot \mathbf{n}\|_{L^2(e)}^2 + \frac{1}{4} \|[\mathbf{a}^\epsilon \nabla v_{h,H} \cdot \mathbf{n}]\|_{L^2(e)}^2 \right). \end{aligned}$$

By the trace inequality, the inverse estimate (5.1), and $\epsilon < H$, we have

$$(5.5) \quad \begin{aligned} \sum_{e \in E} \|(\mathbf{a}^\epsilon \nabla v_H) \cdot \mathbf{n}\|_{L^2(e)}^2 &= \|(\mathbf{a}^\epsilon \nabla v_H) \cdot \mathbf{n}\|_{L^2(E)}^2 \\ &\leq C \left(\frac{1}{H_E} \|\nabla v_H\|_{L^2(K_E)}^2 + \|\nabla v_H\|_{L^2(K_E)} \|\nabla^2 v_H\|_{L^2(K_E)} \right) \\ &\leq \frac{C_1}{\epsilon} \|(\mathbf{a}^\epsilon)^{1/2} \nabla v_H\|_{L^2(K_E)}^2, \end{aligned}$$

where $K_E \in \mathcal{M}_H$ is the element containing E . Therefore, from (5.4) and (5.5), it follows that

$$\begin{aligned} A_\beta(v_{h,H}, v_{h,H}) &\geq \|v_{h,H}\|_{1,h,H}^2 - \sum_{e \in \Gamma_h} \frac{\gamma_0}{2\epsilon} \| [v_{h,H}] \|_{L^2(e)}^2 \\ &\quad - \frac{6C_1}{\gamma_0} \|v_H\|_{1,H}^2 - \frac{3}{2\gamma_0\gamma_1} \sum_{e \in \Gamma_h} \gamma_1 \epsilon \|[\mathbf{a}^\epsilon \nabla v_{h,H} \cdot \mathbf{n}]\|_{L^2(e)}^2 \\ &\geq \|v_{h,H}\|_{1,h,H}^2 - \max \left(\frac{1}{2}, \frac{6C_1\gamma_1}{\gamma_0\gamma_1}, \frac{3}{2\gamma_0\gamma_1} \right) \|v_{h,H}\|_{1,h,H}^2. \end{aligned}$$

Noting that $\gamma_1 \lesssim 1$, there exists a constant $\alpha_0 > 0$ independent of h, H, ϵ such that if $\gamma_0\gamma_1 \geq \alpha_0$ then $\max \left(\frac{6C_1\gamma_1}{\gamma_0\gamma_1}, \frac{3}{2\gamma_0\gamma_1} \right) \leq \frac{1}{2}$. This completes the proof of the Lemma. \square

The following lemma is an analogue of the Strang's lemma for nonconforming finite element methods.

Lemma 5.3. *There exists a constant α_0 independent of ϵ, h, H , and the penalty parameters such that for $0 < \gamma_1 \lesssim 1$, $\gamma_0 \geq \alpha_0/\gamma_1$, the following error estimate holds:*

$$(5.6) \quad \begin{aligned} &\|u_\epsilon - u_{h,H}\|_{1,h,H} \\ &\lesssim \inf_{v_{h,H} \in V_{h,H}} \|u_\epsilon - v_{h,H}\|_{1,h,H} + \sup_{w_{h,H} \in V_{h,H}} \frac{|\int_\Omega f w_{h,H} dx - A_\beta(u_\epsilon, w_{h,H})|}{\|w_{h,H}\|_{1,h,H}}. \end{aligned}$$

Proof. For any $v_{h,H} \in V_{h,H}$, from Lemma 5.2, (5.3), (2.14), and (5.2), we have, for $0 <$

$\gamma_1 \lesssim 1$ and $\gamma_0 \geq \alpha_0/\gamma_1$,

$$\begin{aligned}
\| \|u_{h,H} - v_{h,H}\| \|_{1,h,H}^2 &\lesssim A_\beta(u_{h,H} - v_{h,H}, u_{h,H} - v_{h,H}) \\
&= (f, u_{h,H} - v_{h,H}) - A_\beta(v_{h,H}, u_{h,H} - v_{h,H}) \\
&= (f, u_{h,H} - v_{h,H}) - A_\beta(u_\epsilon, u_{h,H} - v_{h,H}) + A_\beta(u_\epsilon - v_{h,H}, u_{h,H} - v_{h,H}) \\
&\lesssim (f, u_{h,H} - v_{h,H}) - A_\beta(u_\epsilon, u_{h,H} - v_{h,H}) + \| \|u_\epsilon - v_{h,H}\| \|_{1,h,H} \| \|u_{h,H} - v_{h,H}\| \|_{1,h,H}.
\end{aligned}$$

Hence

$$\begin{aligned}
\| \|u_\epsilon - u_{h,H}\| \|_{1,h,H} &\leq \| \|u_\epsilon - v_{h,H}\| \|_{1,h,H} + \| \|u_{h,H} - v_{h,H}\| \|_{1,h,H} \\
&\lesssim \| \|u_\epsilon - v_{h,H}\| \|_{1,h,H} + \frac{|(f, u_{h,H} - v_{h,H}) - A_\beta(u_\epsilon, u_{h,H} - v_{h,H})|}{\| \|u_{h,H} - v_{h,H}\| \|_{1,h,H}}
\end{aligned}$$

which yields the error estimate (5.6). This completes the proof. \square

Now, we are ready to present the main result of the paper which gives the error estimate in the norm $\| \cdot \|_{1,h,H}$ for the FE-MsFEM.

Theorem 5.4. *Assume that the penalty parameter $0 < \gamma_1 \lesssim 1$ and $\gamma_0 \geq \alpha_0/\gamma_1$. Then the following error estimate holds:*

$$\begin{aligned}
\| \|u_\epsilon - u_{h,H}\| \|_{1,h,H} &\lesssim \left(\sqrt{\epsilon} + \frac{\epsilon}{H} + \frac{h}{\epsilon} |\Omega_1|^{1/2} \right) |u_0|_{W^{1,\infty}(\Omega)} + H \|f\|_{L^2(\Omega)} \\
&\quad + \frac{H^2 |u_0|_{H^2(\Omega_\Gamma)}}{\sqrt{\epsilon} \sqrt{|\Omega_\Gamma|}} + \epsilon^2 \|\nabla f\|_{L^2(\Omega_\Gamma)},
\end{aligned}$$

where Ω_Γ is defined in (2.18).

Remark 5.1. (a) *The error bound consists of three parts: the first part of order $O(\sqrt{\epsilon} + \frac{\epsilon}{H} + H)$ from the oversampling MsFE approximation in Ω_2 , the second part of order $O\left(\frac{h}{\epsilon} |\Omega_1|^{1/2}\right)$ from the FE approximation in Ω_1 , and the third part $\frac{H^2 |u_0|_{H^2(\Omega_\Gamma)}}{\sqrt{\epsilon} \sqrt{|\Omega_\Gamma|}} + \epsilon^2 \|\nabla f\|_{L^2(\Omega_\Gamma)}$ from the penalizations on Γ .*

(b) *Suppose that the interface Γ is chosen such that $\text{dist}(\Gamma, \partial\Omega) = O(H)$. If the average value*

$$(5.7) \quad \frac{|u_0|_{H^2(\Omega_\Gamma)}}{\sqrt{|\Omega_\Gamma|}} \lesssim 1,$$

then we have

$$\| \|u_\epsilon - u_{h,H}\| \|_{1,h,H} \lesssim \sqrt{\epsilon} + \frac{\epsilon}{H} + H + \frac{hH^{1/2}}{\epsilon} + \frac{H^2}{\sqrt{\epsilon}}.$$

In this case, we may choose $H \approx \sqrt{\epsilon}$ and $h \approx \epsilon^{5/4}$ to ensure that $\| \|u_\epsilon - u_{h,H}\| \|_{1,h,H} \lesssim \sqrt{\epsilon}$. The condition (5.7) may be checked by using the standard singularity decomposition results

for elliptic problems on polygonal domains [41, 17]. For example, we may show for the two dimensional case ($n=2$) that, if the inner angles of the polygon Ω are less than $\frac{2}{3}\pi$, then (5.7) holds.

Proof. According to Lemma 5.3, the proof is divided into two parts. The first part is devoted to estimating the interpolation error and the second part to estimating the non-conforming error.

Part 1. Interpolation error estimate. We set $v_{h,H}$ as $v_{h,H}|_{\Omega_1} = \hat{u}_h, v_{h,H}|_{\Omega_2} = \psi_H$, where $\hat{u}_h := Z_h u_1$ and ψ_H are defined in Lemma 4.7 and Lemma 4.3 respectively. We are going to estimate $\|u_\epsilon - v_{h,H}\|_{1,h,H}$, i.e., to estimate each term in its definition (cf. (2.21)). First, from Lemmas 4.4, 4.7, we have

$$(5.8) \quad \left(\|u_\epsilon - v_{h,H}\|_{1,H}^2 + \|(\mathbf{a}^\epsilon)^{1/2} \nabla(u_\epsilon - v_{h,H})\|_{L^2(\Omega_1)}^2 \right)^{1/2} \\ \lesssim H |u_0|_{H^2(\Omega)} + \sqrt{\epsilon} |u_0|_{W^{1,\infty}(\Omega)} + \frac{\epsilon}{H} |u_0|_{W^{1,\infty}(\Omega_2)} + \frac{h}{\epsilon} |\Omega_1|^{1/2} |u_0|_{W^{1,\infty}(\Omega_1)}.$$

Further, since $[u_\epsilon] = 0$ and $[u_1] = 0$, it is easy to see that

$$\sum_{e \in \Gamma_h} \frac{\gamma_0}{\epsilon} \int_e [u_\epsilon - v_{h,H}]^2 = \sum_{e \in \Gamma_h} \frac{\gamma_0}{\epsilon} \int_e [u_1 - v_{h,H}]^2 \\ \leq \sum_{E \in \Gamma_H} \frac{\gamma_0}{\epsilon} \int_E (u_1 - \psi_H)^2 + \sum_{e \in \Gamma_h} \frac{\gamma_0}{\epsilon} \int_e (u_1 - \hat{u}_h)^2.$$

By the trace inequality, we have

$$\int_E (u_1 - \psi_H)^2 \lesssim H^{-1} \|u_1 - \psi_H\|_{L^2(K)}^2 + \|u_1 - \psi_H\|_{L^2(K)} \|\nabla(u_1 - \psi_H)\|_{L^2(K)}.$$

Hence, taking a summation over Γ_H , yields

$$\sum_{E \in \Gamma_H} \frac{\gamma_0}{\epsilon} \int_E (u_1 - \psi_H)^2 \lesssim \frac{1}{H\epsilon} \sum_{K \in K_{\Gamma_H}} \|u_1 - \psi_H\|_{L^2(K)}^2 \\ + \frac{1}{\epsilon} \left(\sum_{K \in K_{\Gamma_H}} \|u_1 - \psi_H\|_{L^2(K)}^2 \right)^{1/2} \left(\sum_{K \in K_{\Gamma_H}} \|\nabla(u_1 - \psi_H)\|_{L^2(K)}^2 \right)^{1/2}.$$

Thus, from from (3.7), (4.13), and (4.14), it follows that

$$\sum_{E \in \Gamma_H} \frac{\gamma_0}{\epsilon} \int_E (u_\epsilon - \psi_H)^2 \lesssim \epsilon |u_0|_{W^{1,\infty}(\Omega_{\Gamma_H})}^2 + \frac{H^3}{\epsilon} |u_0|_{H^2(\Omega_{\Gamma_H})}^2.$$

Further, by the trace inequality, from Lemma 4.5, it follows

$$\begin{aligned}
& \sum_{e \in \Gamma_h} \frac{\gamma_0}{\epsilon} \int_e (u_1 - \hat{u}_h)^2 \\
& \lesssim \frac{1}{\epsilon} \sum_{e \in \Gamma_h} \left(h^{-1} \|u_1 - \hat{u}_h\|_{L^2(K_e)}^2 + \|u_1 - \hat{u}_h\|_{L^2(K_e)} \|\nabla(u_1 - \hat{u}_h)\|_{L^2(K_e)} \right) \\
& \lesssim \frac{h^3}{\epsilon} |u_1|_{H^2(\Omega_{\Gamma_h})}^2,
\end{aligned}$$

where Ω_{Γ_h} is defined in (2.19), and, in order to ensure the last inequality, for any vertex of elements in K_{Γ_h} , we have chosen the corresponding edge/face in the definition of Scott-Zhang interpolation to be an edge/face of some element in K_{Γ_h} . Therefore, from the above two estimates and Lemma 3.5, we have

$$\begin{aligned}
(5.9) \quad \sum_{e \in \Gamma_h} \frac{\gamma_0}{\epsilon} \int_e [u_\epsilon - v_{h,H}]^2 & \lesssim \frac{H^3}{\epsilon} |u_0|_{H^2(\Omega_\Gamma)}^2 + h^2 |u_0|_{H^2(\Omega)}^2 \\
& \quad + \epsilon |u_0|_{W^{1,\infty}(\Omega)}^2 + \epsilon^4 \|\nabla f\|_{L^2(\Omega_\Gamma)}^2.
\end{aligned}$$

Next, we estimate the term

$$\sum_{e \in \Gamma_h} \frac{\epsilon}{\gamma_0} \|\{\mathbf{a}^\epsilon \nabla(u_\epsilon - v_{h,H}) \cdot \mathbf{n}\}\|_{L^2(e)}^2.$$

It is easy to see that

$$\begin{aligned}
\sum_{e \in \Gamma_h} \frac{\epsilon}{\gamma_0} \|\{\mathbf{a}^\epsilon \nabla(u_\epsilon - v_{h,H}) \cdot \mathbf{n}\}\|_{L^2(e)}^2 & \lesssim \sum_{E \in \Gamma_H} \frac{\epsilon}{\gamma_0} \|\mathbf{a}^\epsilon \nabla(u_\epsilon - \psi_H) \cdot \mathbf{n}\|_{L^2(E)}^2 \\
& \quad + \sum_{e \in \Gamma_h} \frac{\epsilon}{\gamma_0} \|\mathbf{a}^\epsilon \nabla(u_\epsilon - \hat{u}_h) \cdot \mathbf{n}\|_{L^2(e)}^2.
\end{aligned}$$

By the trace inequality, we have

$$\begin{aligned}
& \|\mathbf{a}^\epsilon \nabla(u_\epsilon - \psi_H) \cdot \mathbf{n}\|_{L^2(E)}^2 \lesssim \|\nabla(u_\epsilon - u_1) \cdot \mathbf{n}\|_{L^2(E)}^2 + \|\nabla(u_1 - \psi_H) \cdot \mathbf{n}\|_{L^2(E)}^2 \\
& \leq H^{-1} \|\nabla(u_\epsilon - u_1)\|_{L^2(K)}^2 + \|\nabla(u_\epsilon - u_1)\|_{L^2(K)} \|\nabla^2(u_\epsilon - u_1)\|_{L^2(K)} \\
& \quad + H^{-1} \|\nabla(u_1 - \psi_H)\|_{L^2(K)}^2 + \|\nabla(u_1 - \psi_H)\|_{L^2(K)} \|\nabla^2(u_1 - \psi_H)\|_{L^2(K)}.
\end{aligned}$$

Hence, a summation over Γ_H follows that

$$\begin{aligned}
& \sum_{E \in \Gamma_H} \frac{\epsilon}{\gamma_0} \|\mathbf{a}^\epsilon \nabla(u_\epsilon - \psi_H) \cdot \mathbf{n}\|_{L^2(E)}^2 \\
& \lesssim \epsilon H^{-1} \|\nabla(u_\epsilon - u_1)\|_{L^2(\Omega_{\Gamma_H})}^2 + \epsilon H^{-1} \sum_{K \in K_{\Gamma_H}} \|\nabla(u_1 - \psi_H)\|_{L^2(K)}^2 \\
& \quad + \epsilon \|\nabla(u_\epsilon - u_1)\|_{L^2(\Omega_{\Gamma_H})} \|\nabla^2(u_\epsilon - u_1)\|_{L^2(\Omega_{\Gamma_H})} \\
& \quad + \epsilon \left(\sum_{K \in K_{\Gamma_H}} \|\nabla(u_1 - \psi_H)\|_{L^2(K)}^2 \right)^{1/2} \left(\sum_{K \in K_{\Gamma_H}} \|\nabla^2(u_1 - \psi_H)\|_{L^2(K)}^2 \right)^{1/2}.
\end{aligned}$$

Therefore, it follows that from Theorems 3.1, 3.4 and Lemma 4.3,

$$\begin{aligned}
(5.10) \quad & \sum_{E \in \Gamma_H} \frac{\epsilon}{\gamma_0} \|\mathbf{a}^\epsilon \nabla(u_\epsilon - \psi_H) \cdot \mathbf{n}\|_{L^2(e)}^2 \lesssim (H + \epsilon)^2 |u_0|_{H^2(\Omega)}^2 \\
& \quad + \epsilon |u_0|_{W^{1,\infty}(\Omega)}^2 + \epsilon^4 \|\nabla f\|_{L^2(\Omega_\Gamma)}^2.
\end{aligned}$$

Similarly, by the trace inequality, we have

$$\begin{aligned}
& \sum_{e \in \Gamma_h} \frac{\epsilon}{\gamma_0} \|\mathbf{a}^\epsilon \nabla(u_\epsilon - \hat{u}_h) \cdot \mathbf{n}\|_{L^2(e)}^2 \\
& \lesssim \epsilon \sum_{E \in \Gamma_H} \|\mathbf{a}^\epsilon \nabla(u_\epsilon - u_1) \cdot \mathbf{n}\|_{L^2(E)}^2 + \epsilon \sum_{e \in \Gamma_h} \|\mathbf{a}^\epsilon \nabla(u_1 - \hat{u}_h) \cdot \mathbf{n}\|_{L^2(e)}^2 \\
& \lesssim \epsilon H^{-1} \|\nabla(u_\epsilon - u_1)\|_{L^2(\Omega_{\Gamma_H})}^2 + \epsilon \|\nabla(u_\epsilon - u_1)\|_{L^2(\Omega_{\Gamma_H})} \|\nabla^2(u_\epsilon - u_1)\|_{L^2(\Omega_{\Gamma_H})} \\
& \quad + \epsilon h^{-1} \|\nabla(u_1 - \hat{u}_h)\|_{L^2(\Omega_{\Gamma_h})}^2 + \epsilon \|\nabla(u_1 - \hat{u}_h)\|_{L^2(\Omega_{\Gamma_h})} \|\nabla^2 u_1\|_{L^2(\Omega_{\Gamma_h})}.
\end{aligned}$$

Thus, from Theorems 3.1,3.4 and Lemmas 3.5, 4.7, it follows that

$$\begin{aligned}
(5.11) \quad & \sum_{e \in \Gamma_h} \frac{\epsilon}{\gamma_0} \|\mathbf{a}^\epsilon \nabla(u_\epsilon - \hat{u}_h) \cdot \mathbf{n}\|_{L^2(e)}^2 \\
& \lesssim \epsilon^2 |u_0|_{H^2(\Omega)}^2 + \epsilon |u_0|_{W^{1,\infty}(\Omega)}^2 + \epsilon^4 \|\nabla f\|_{L^2(\Omega_\Gamma)}^2.
\end{aligned}$$

It is obvious that a same argument as above can be used to get the same error bound for the term

$$\sum_{e \in \Gamma_h} \gamma_1 \epsilon \|\mathbf{a}^\epsilon \nabla(u_\epsilon - v_{h,H}) \cdot \mathbf{n}\|_{L^2(e)}^2.$$

Thus, it follows from (5.8)–(5.11) that

$$\begin{aligned}
(5.12) \quad & \inf_{v_{h,H} \in V_{h,H}} \|u_\epsilon - v_{h,H}\|_{1,h,H} \lesssim H |u_0|_{H^2(\Omega)} + \left(\sqrt{\epsilon} + \frac{\epsilon}{H} \right) |u_0|_{W^{1,\infty}(\Omega)} \\
& \quad + \frac{h}{\epsilon} |\Omega_1|^{1/2} |u_0|_{W^{1,\infty}(\Omega_1)} + \frac{H^{3/2}}{\sqrt{\epsilon}} |u_0|_{H^2(\Omega_\Gamma)} + \epsilon^2 \|\nabla f\|_{L^2(\Omega_\Gamma)}.
\end{aligned}$$

Part 2. The non-conforming error estimate. Define

$$\mathcal{E}_H^I := \text{set of all interior edges/faces of } \mathcal{M}_H .$$

For any $w_{h,H} \in V_{h,H}$, noticing that $\partial\Omega_2/\Gamma$ is empty, it is easy to see

$$\begin{aligned} (f, w_{h,H}) &= (f, w_h)_{\Omega_1} + (f, w_H)_{\Omega_2} = (-\nabla \cdot (\mathbf{a}^\epsilon \nabla u_\epsilon), w_h)_{\Omega_1} + (-\nabla \cdot (\mathbf{a}^\epsilon \nabla u_\epsilon), w_H)_{\Omega_2} \\ &= (\mathbf{a}^\epsilon \nabla u_\epsilon, \nabla w_h)_{\Omega_1} - \int_\Gamma \mathbf{a}^\epsilon \nabla u_\epsilon \cdot \mathbf{n} w_h \\ &\quad + \sum_{K \in \mathcal{M}_H} \left((\mathbf{a}^\epsilon \nabla u_\epsilon, \nabla w_H)_K - \int_{\partial K} \mathbf{a}^\epsilon \nabla u_\epsilon \cdot \mathbf{n}_K w_H \right) \\ &= (\mathbf{a}^\epsilon \nabla u_\epsilon, \nabla w_h)_{\Omega_1} - \sum_{e \in \Gamma_h} \int_e \mathbf{a}^\epsilon \nabla u_\epsilon \cdot \mathbf{n} (w_h - w_H) \\ &\quad + \sum_{K \in \mathcal{M}_H} (\mathbf{a}^\epsilon \nabla u_\epsilon, \nabla w_H)_K - \sum_{E \in \mathcal{E}_H^I} \int_E \mathbf{a}^\epsilon \nabla u_\epsilon \cdot \mathbf{n}_E [w_H]. \end{aligned}$$

Here the unit normal vector \mathbf{n}_E is oriented from K to K' and the jump $[v]$ of v on an interior side $E = \partial K \cap \partial K' \in \mathcal{E}_H^I$ is defined as $[v] := v|_K - v|_{K'}$. Furthermore, by the definition of A_β , it follows that

$$A_\beta(u_\epsilon, w_{h,H}) = (\mathbf{a}^\epsilon \nabla u_\epsilon, \nabla w_h)_{\Omega_1} - \sum_{e \in \Gamma_h} \int_e \mathbf{a}^\epsilon \nabla u_\epsilon \cdot \mathbf{n} (w_h - w_H) + \sum_{K \in \mathcal{M}_H} (\mathbf{a}^\epsilon \nabla u_\epsilon, \nabla w_H)_K.$$

Thus, we have

$$\begin{aligned} (f, w_{h,H}) - A_\beta(u_\epsilon, w_{h,H}) &= - \sum_{E \in \mathcal{E}_H^I} \int_E \mathbf{a}^\epsilon \nabla u_\epsilon \cdot \mathbf{n}_E [w_H] \\ &= - \sum_{E \in \mathcal{E}_H^I} \int_E \mathbf{a}^\epsilon \nabla u_\epsilon \cdot \mathbf{n}_E [w_H - \Pi_H w_H] \\ &= - \sum_{K \in \mathcal{M}_H} \int_{\partial K} \mathbf{a}^\epsilon \nabla u_\epsilon \cdot \mathbf{n}_K (w_H - \Pi_H w_H) - \sum_{E \in \Gamma_H} \int_E \mathbf{a}^\epsilon \nabla u_\epsilon \cdot \mathbf{n} (w_H - \Pi_H w_H) \\ &:= R_1 + R_2. \end{aligned}$$

Since

$$R_1 = \int_{\Omega_2} f(w_H - \Pi_H w_H) - \sum_{K \in \mathcal{M}_H} \int_K \mathbf{a}^\epsilon \nabla u_\epsilon \nabla (w_H - \Pi_H w_H),$$

we can estimate R_1 by following [26, Chapter 6], or [15, Chapter 9], or the proof presented in [28, Theorem 3.1], and obtain

$$(5.13) \quad |R_1| \leq C \left(\epsilon |u_0|_{H^2(\Omega_2)} + \left(\sqrt{\epsilon} + \frac{\epsilon}{H} \right) |u_0|_{W^{1,\infty}(\Omega_2)} + \epsilon \|f\|_{L^2(\Omega_2)} \right) \|w_H\|_{1,H}.$$

Next, we consider the second term R_2 . For any $w_H \in X_H$, it is easy to check that (see [15, 28])

$$w_H = \Pi_K w_H + \epsilon \chi^j \frac{\partial(\Pi_K w_H)}{\partial x_j} + \epsilon \theta_\epsilon^S \quad \text{in } S,$$

where $\theta_\epsilon^S \in H^1(S)$ is the boundary corrector given by

$$-\nabla \cdot (\mathbf{a}^\epsilon \nabla \theta_\epsilon^S) = 0 \quad \text{in } S, \quad \theta_\epsilon^S|_{\partial S} = -\chi^j \frac{\partial(\Pi_K w_H)}{\partial x_j}.$$

By the Maximum Principle, we have

$$\|\theta_\epsilon^S\|_{L^\infty(S)} \leq C \|\nabla \Pi_K w_H\|_{L^\infty(S)}.$$

Thus, from Lemma 4.1, we obtain

$$\begin{aligned} \|w_H - \Pi_K w_H\|_{L^\infty(\partial K)} &\lesssim \epsilon \|\nabla \Pi_K w_H\|_{L^\infty(S)} \lesssim \epsilon \|\nabla \Pi_K w_H\|_{L^\infty(K)} \\ &\lesssim \epsilon H^{-n/2} \|\nabla \Pi_K w_H\|_{L^2(K)} \lesssim \epsilon H^{-n/2} \|\nabla w_H\|_{L^2(K)}, \end{aligned}$$

which yields

$$\begin{aligned} |R_2| &\lesssim \sum_{E \in \Gamma_H} \|\nabla u_\epsilon\|_{L^2(E)} \|w_H - \Pi_H w_H\|_{L^2(E)} \\ &\lesssim \|\nabla u_\epsilon\|_{L^2(\Gamma)} \left(\sum_{E \in \Gamma_H} H^{n-1} \|w_H - \Pi_H w_H\|_{L^\infty(E)}^2 \right)^{1/2} \\ &\lesssim \|\nabla u_\epsilon\|_{L^2(\Gamma)} \left(\sum_{K \in K_{\Gamma_H}} \epsilon^2 H^{-1} \|\nabla w_H\|_{L^2(K)}^2 \right)^{1/2} \\ &\lesssim \epsilon H^{-1/2} \|\nabla u_\epsilon\|_{L^2(\Gamma)} \|w_H\|_{1,H}. \end{aligned}$$

On the other hand, by use of the trace inequality, it follows from Theorems 3.1, 3.4, and Lemma 3.3 that

$$\begin{aligned} \|\nabla u_\epsilon\|_{L^2(\Gamma)}^2 &\leq \|\nabla(u_\epsilon - u_1)\|_{L^2(\Gamma)}^2 + \|\nabla u_0\|_{L^2(\Gamma)}^2 + \left\| \nabla \left(\epsilon \chi^i \frac{\partial u_0}{\partial x_j} \right) \right\|_{L^2(\Gamma)}^2 \\ &\lesssim \sum_{K \in K_{\Gamma_H}} \left(H^{-1} \|\nabla(u_\epsilon - u_1)\|_{L^2(K)}^2 + \|\nabla(u_\epsilon - u_1)\|_{L^2(K)} \|u_\epsilon - u_1\|_{H^2(K)} \right) \\ &\quad + |u_0|_{W^{1,\infty}(\Omega)}^2 + \epsilon^2 \sum_{K \in K_{\Gamma_H}} \left(H^{-1} |u_0|_{H^2(K)}^2 + |u_0|_{H^2(K)} |u_0|_{H^3(K)} \right) \\ &\lesssim \epsilon |u_0|_{H^2(\Omega)}^2 + |u_0|_{W^{1,\infty}(\Omega)}^2 + \epsilon^3 \|\nabla f\|_{L^2(\Omega_\Gamma)}^2. \end{aligned}$$

Therefore

$$(5.14) \quad |R_2| \lesssim \left(\epsilon |u_0|_{H^2(\Omega)} + \sqrt{\epsilon} |u_0|_{W^{1,\infty}(\Omega)} + \epsilon^2 \|\nabla f\|_{L^2(\Omega_\Gamma)} \right) \|w_H\|_{1,H}.$$

It follows from (5.13) and (5.14) that the non-conforming error in Lemma 5.3

$$\begin{aligned} & \sup_{w_{h,H} \in V_{h,H}} \frac{|\int_{\Omega} f w_{h,H} - A_{\beta}(u, w_{h,H})|}{\|w_{h,H}\|_{1,h,H}} \\ & \lesssim \epsilon |u_0|_{H^2(\Omega)} + \left(\sqrt{\epsilon} + \frac{\epsilon}{H}\right) |u_0|_{W^{1,\infty}(\Omega)} + \epsilon \|f\|_{L^2(\Omega)} + \epsilon^2 \|\nabla f\|_{L^2(\Omega_{\Gamma})}, \end{aligned}$$

which, combining with (5.12), (5.6), and (3.5), completes the proof. \square

6 Numerical tests

In this section, we first demonstrate the performance of the proposed FE-MsFEM by solving the model problem (1.1) with periodic and randomly generated coefficients respectively, and then show the ability of the FE-MsFEM to solve two multiscale elliptic problems with high-contrast channels. In all computations we do not assume that the diffusion coefficient values are available outside of the research domain. In order to illustrate the performance of our method, we also implement two other kinds of methods. The first is the standard MsFEM. The second one is a mixed basis MsFEM which use the oversampling multiscale basis inside the domain but away from the boundary, while use the standard MsFEM basis near the boundary. By this way, the mixed basis MsFEM doesn't need to use the outside information.

For the methods FE-MsFEM and mixed basis MsFEM, the triangulation may be done by the following three steps.

- First, we triangulate the domain Ω with a coarse mesh whose mesh size H is much bigger than ϵ .
- Secondly, we choose the union of coarse-grid elements adjacent to the boundary $\partial\Omega$ (and the channels if exist) as Ω_1 and denote $\Omega \setminus \overline{\Omega_1}$ by Ω_2 . For example, in our tests, we choose two layers of coarse-grid elements (and the coarse-grid elements containing the channels if exist) to form the domain Ω_1 . Hence the distance of Γ away from $\partial\Omega$ is $2H$.
- Finally, in Ω_2 , we use the oversampling MsFEM basis on coarse-grid elements. While, in Ω_1 we use the traditional linear FEM basis on a fine mesh for the FE-MsFEM, or use the standard MsFEM basis on coarse-grid elements for the mixed basis MsFEM. In our tests, we fix the mesh size of the fine mesh $h = 1/1024$ which is small enough to resolve the smallest scale of oscillations.

Please see Fig. 1 for a sample triangulation.

Since there are no exact solutions to the problems considered here, we will solve them on a very fine mesh with mesh size $h_f = 1/2048$ by use of the traditional linear finite element method, and consider their numerical solutions as the “exact” solutions which are denoted as u_e . Denoting by u_h the numerical solutions computed by the methods

considered in this section, we measure the relative errors in the L^2 , L^∞ and energy norms as following

$$\frac{\|u_h - u_e\|_{L^2}}{\|u_e\|_{L^2}}, \frac{\|u_h - u_e\|_{L^\infty}}{\|u_e\|_{L^\infty}}, \frac{\|u_h - u_e\|_E}{\|u_e\|_E}.$$

In all tests, for simplicity, the penalty parameters in our FE-MsFEM are chosen as $\gamma_0 = 20$ and $\gamma_1 = 0.1$. The coefficient \mathbf{a}^ϵ is chosen as the form $\mathbf{a}^\epsilon = a^\epsilon I$ where a^ϵ is a scalar function and I is the 2 by 2 identity matrix.

6.1 Application to elliptic problems with highly oscillating coefficients

We first consider the model problem (1.1) in the squared domain $\Omega = (0, 1) \times (0, 1)$. Assume that $f = 1$ and the coefficient $\mathbf{a}^\epsilon(x_1, x_2)$ has the following periodic form

$$(6.1) \quad a^\epsilon(x_1, x_2) = \frac{2 + 1.8 \sin(2\pi x_1/\epsilon)}{2 + 1.8 \cos(2\pi x_2/\epsilon)} + \frac{2 + 1.8 \sin(2\pi x_2/\epsilon)}{2 + 1.8 \sin(2\pi x_1/\epsilon)}.$$

where we fix $\epsilon = 1/100$. In our FE-MsFEM, we consider two choices of the parameter ρ . The first choice is $\rho = \epsilon$ as stated in our theoretical analysis, while the other one $\rho = h$, the size of the fine mesh. The second choice is useful when the scales are non-separable. We first choose $H = 1/32$ and report the relative errors in the L^2 , L^∞ and energy norms in Table 1. We can see that the FE-MsFEMs give the most accurate results among the

Table 1: Relative errors in the L^2 , L^∞ and energy norms for the model problem with periodic coefficient given by (6.1). $\epsilon = 1/100$, $H = 1/32$, $h = 1/1024$, $\gamma_0 = 20$, $\gamma_1 = 0.1$.

Relative Error	L^2	L^∞	Energy norm
MsFEM	0.7263e-01	0.7157e-01	0.2560e-00
Mixed basis MsFEM	0.3422e-01	0.3637e-01	0.1714e-00
FE-MsFEM $\rho = \epsilon$	0.1238e-01	0.1334e-01	0.5159e-01
FE-MsFEM $\rho = h$	0.1252e-01	0.1344e-01	0.4840e-01

methods considered here. Especially, when we take $\rho = h$, the FE-MsFEM still works well.

The following numerical experiment is to show the coarse mesh size H plays a role as that describing in the Theorem 5.4. We fix $h = 1/1024$ and $\epsilon = 1/100$. Three kinds of coarse mesh size are chosen. The first one, $H = 1/64$, is denoted as 64×16 ; the second one, $H = 1/32$, is denoted as 32×32 ; the last one, $H = 1/16$, is denoted as 16×64 . The results are shown in Table 2. From the table, it is easy to see that as H goes larger, the relative error in energy norm goes lower first and goes higher later, which is coincided with the theoretical results in Theorem 5.4.

Next we simulate the model problem with a random coefficient which is generated by using the random log-normal permeability field $\mathbf{a}^\epsilon(x)$ by using the moving ellipse average technique [20] with the variance of the logarithm of the permeability $\sigma^2 = 1.5$, and

Table 2: Relative errors of the FE-MsFEM with $H = 1/64, 1/32$, and $1/16$, respectively, for the model problem with periodic coefficient given by (6.1). $\rho = \epsilon = 1/100$, $h = 1/1024$, $\gamma_0 = 20$, $\gamma_1 = 0.1$.

Relative Error	L^2	L^∞	Energy norm
64×16	0.1100e-01	0.1502e-01	0.9342e-01
32×32	0.1186e-01	0.1290e-01	0.5159e-01
16×64	0.1240e-01	0.1795e-01	0.6593e-01

the correlation lengths $l_1 = l_2 = 0.01$ (isotropic heterogeneity) in x_1 and x_2 directions, respectively. The ratio of maximum to minimum of one realization of the resulting permeability field in our numerical experiments is $1.6137e+05$. One realization of the resulting permeability field in our numerical experiments is depicted in Fig. 2. We also compare

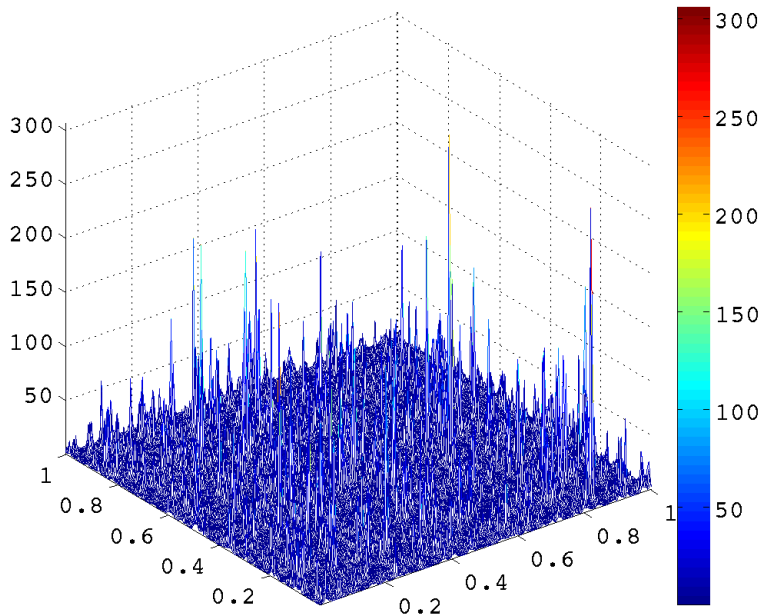


Figure 2: The random log-normal permeability field $a^\epsilon(x)$. The ratio of maximum to minimum is $1.6137e+05$.

three kinds of methods including the standard MsFEM, the Mixed basis MsFEM and the FE-MsFEM. In this test, we set $H = 1/32$ and $\rho = h$ since there is no explicit ϵ in this example. The relative errors for the three methods are listed in Table 3. From the table, we can also see that the FE-MsFEM gives the most accurate results among the methods considered here.

Table 3: Relative errors in the L^2 , L^∞ and energy norms for the model problem with random coefficient as shown in Figure 2. $H = 1/32, \rho = h = 1/1024, \gamma_0 = 20, \gamma_1 = 0.1$.

Relative Error	L^2	L^∞	Energy norm
MsFEM	0.3690e-00	0.3731e-00	0.6014e-00
Mixed basis MsFEM	0.1119e-00	0.1857e-00	0.4770e-00
FE-MsFEM	0.2635e-01	0.8351e-01	0.2975e-00

6.2 Application to multiscale problems with high-contrast channels

In this subsection, we use the introduced FE-MsFEM to solve two elliptic multiscale problems which have high-contrast channels inside the domain.

In the first example, the coefficient \mathbf{a}^ϵ is characterized by a fine and long-ranged high-permeability channel, which is set by the following way. The example utilizes the periodic coefficient a^ϵ in (6.1) as the background, while changing the values on a narrow and long channel that defined from $(0.08, 0.49)$ to $(0.92, 0.51)$ with new value $a^\epsilon = 10^5$ (See Fig. 3). For this problem, the “exact ” solution is difficult to be obtained due to the singularities

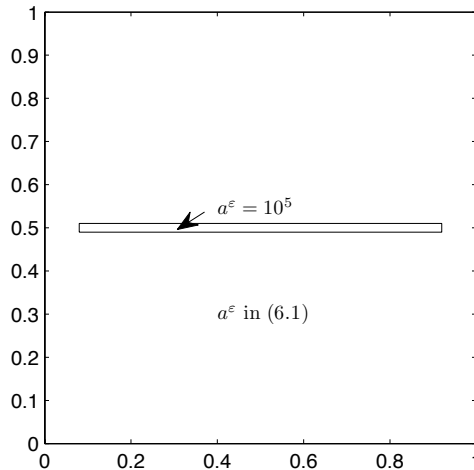


Figure 3: Permeability field

near the corners of the high contrast channel. Our direct numerical simulation shows that the gradient values are large near the corners of the channel. We set $H = 1/32$ and $\rho = \epsilon = 1/100$. The results are presented in Table 4 where the relative errors in L^2, L^∞ norms as well as energy norm are shown. We observe that the FE-MsFEM performs better than other methods.

In the second example, we use the coefficient depicted in Fig 4 that corresponds to a coefficient with background one and high permeability channels and inclusions with

Table 4: Relative errors for the model problem with the permeability depicted in Fig.3. $\rho = \epsilon = 1/100$, $H = 1/32$, $h = 1/1024$, $\gamma_0 = 20$, $\gamma_1 = 0.1$.

Relative Error	L^2	L^∞	Energy norm
MsFEM	0.1640e-00	0.2187e-00	0.3773e-00
Mixed basis MsFEM	0.5415e-01	0.2552e-00	0.2977e-00
FE-MsFEM	0.1127e-01	0.2090e-01	0.6843e-01

permeability values equal to 10^5 and 8×10^4 respectively. The results are listed in Table 5.

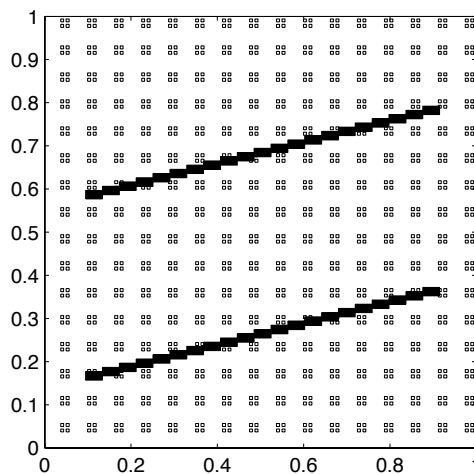


Figure 4: Permeability field: $a^\epsilon = 10^5$ in two channels consisting of dark small rectangles; $a^\epsilon = 8 \times 10^4$ in small square inclusions; $a^\epsilon = 1$ otherwise.

We observe that our FE-MsFEM gives much better results than the other two methods.

7 Conclusions

In this paper, we have developed a new numerical scheme for the elliptic multiscale problems which joints the oversampling MsFEM and the standard FEM together by using the penalty techniques. The idea is first to separate the research domain into two parts Ω_1 and $\Omega_2 = \Omega \setminus \overline{\Omega_1}$ that Ω_1 contains the boundary $\partial\Omega$ where the oversampling MsFEM can not apply, and singular points (or regions) where the oversampling MsFEM is inefficient. Then we apply the standard FEM on a fine mesh of Ω_1 and the oversampling MsFEM on a coarse mesh of Ω_2 . The two methods are jointed on the interface $\Gamma = \partial\Omega_1 \cap \partial\Omega_2$ of the fine and coarse meshes by penalizing the jumps of the function values as well as the fluxes of discrete solutions.

A rigorous and careful analysis has been given for the elliptic equation with periodic

Table 5: Relative errors for the model problem with the permeability depicted in Fig.4. $H = 1/32$, $\rho = h = 1/1024$, $\gamma_0 = 20$, $\gamma_1 = 0.1$.

Relative Error	L^2	L^∞	Energy norm
MsFEM	0.3546e-00	0.4007e-00	0.5943e-00
Mixed basis MsFEM	0.2243e-00	0.2596e-00	0.4997e-00
FE-MsFEM	0.4274e-02	0.1284e-01	0.7566e-01

diffusion coefficient to show that, under some mild assumptions, if Γ is so chosen that $\text{dist}(\Gamma, \partial\Omega) \gtrsim H$, then the H^1 -error of our new method is of order

$$O\left(\sqrt{\epsilon} + \frac{\epsilon}{H} + H + \frac{h}{\epsilon}|\Omega_1| + \frac{H^2}{\sqrt{\epsilon}}\right),$$

which exactly consists of the oversampling MsFE approximation error in Ω_2 , the FE approximation error in Ω_1 , and the error contributed by the penalizations on Γ . Note that, for simplicity, we have only analyzed the linear version of FEM for the discretization on Ω_1 .

Numerical experiments are carried out for the elliptic equations with periodic oscillating or random coefficients, as well as, the multiscale problems with high contrast channels, to verify the theoretical findings and compare the performance of our FE-MsFEM with the standard MsFEM and Mixed basis MsFEM. It is shown that, the FE-MsFEM performs better than the other two methods in all cases and much better in some experiments.

There are several ways to improve further the performance of our FE-MsFEM. First, the linear FEM on Ω_1 can be apparently extended to higher order FEMs to reduce the error term related to Ω_1 . Secondly, since Ω_1 may contains singularities, another interesting project is to consider a combination of adaptive FEM on local refined meshes on Ω_1 and oversampling MsFEM on Ω_2 . Thirdly, based on existence numerical results for oversampling MsFEMs [42], we conjecture that the theoretical assumption of $\text{dist}(\Gamma, \partial\Omega) \gtrsim H$ may be weakened to $\text{dist}(\Gamma, \partial\Omega) \geq C\epsilon$ (at least, in practice) for some constant C . These will be left as future studies.

References

- [1] J. E. AARNES, *On the use of a mixed multiscale finite element method for greater flexibility and increased speed or improved accuracy in reservoir simulation*, SIAM MMS, 2 (2004), pp. 421–439.
- [2] T. ARBOGAST, *Numerical subgrid upscaling of two-phase flow in porous media*, in Numerical Treatment of Multiphase Flows in Porous Media, Z. Chen, R. E. Ewing, and Z. C. Shi, eds., vol. 552 of Lect. Notes Phys., Springer-Verlag, New York, 2000, pp. 35–49.

- [3] —, *Implementation of a locally conservative numerical subgrid upscaling scheme for two-phase darcy flow*, *Comput. Geosci.*, 6 (2002), pp. 453–481.
- [4] T. ARBOGAST, G. PENCHEVA, M. F. WHEELER, AND I. YOTOV, *A multiscale mortar mixed finite element method*, *SIAM MMS*, 6 (2007), pp. 319–346.
- [5] D. ARNOLD, *An interior penalty finite element method with discontinuous elements*, *SIAM J. Numer. Anal.*, 19 (1982), pp. 742–760.
- [6] D. ARNOLD, F. BREZZI, B. COCKBURN, AND D. MARINI, *Unified analysis of discontinuous Galerkin methods for elliptic problems.*, *SIAM J. Numer. Anal.*, 39 (2001), pp. 1749–1779.
- [7] M. AVELLANEDA AND F. LIN, *Compactness methods in the theory of homogenization*, *Comm. Pure Appl. Math.*, 40 (1987), pp. 803–847.
- [8] I. BABUSKA, G. CALOZ, AND J. OSBORN, *Special finite element methods for a class of second order elliptic problems with rough coefficients*, *SIAM J. Numer. Anal.*, 31 (1994), pp. 945–981.
- [9] I. BABUSKA AND J. OSBORN, *Generalized finite element methods: their performance and their relation to mixed methods*, *SIAM J. Numer. Anal.*, 20 (1983), pp. 510–536.
- [10] I. BABUŠKA AND M. ZLÁMAL, *Nonconforming elements in the finite element method with penalty*, *SIAM Journal on Numerical Analysis*, 10 (1973), pp. pp. 863–875.
- [11] G. BAKER, *Finite element methods for elliptic equations using nonconforming elements*, *Math. Comp.*, 31 (1977), pp. 44–59.
- [12] A. BENSOUSSAN, J. L. LIONS, AND G. PAPANICOLAOU, *Asymptotic analysis for periodic structure*, vol. 5 of *Studies in Mathematics and Its Application*, North-Holland Publ., 1978.
- [13] F. BREZZI, L. P. FRANCA, T. J. R. HUGHES, AND A. RUSSO, $b = \int g$, *Comput. Methods Appl. Mech. Engrg.*, 145 (1997), pp. 329–339.
- [14] Z. CHEN AND T. Y. HOU, *A mixed multiscale finite method for elliptic problems with oscillating coefficients*, *Math. Comp.*, 72 (2002), pp. 541–576.
- [15] Z. CHEN AND H. WU, *Selected topics in finite element method*, Science Press, Beijing, 2010.
- [16] Z. CHEN AND X. Y. YUE, *Numerical homogenization of well singularities in the flow transport through heterogeneous porous media*, *SIAM MMS*, 1 (2003), pp. 260–303.
- [17] M. DAUGE, *Elliptic Boundary Value Problems in Corner Domains – Smoothness and Asymptotics of Solutions.*, vol. 1341 of *Lecture Notes in Mathematics*, Springer-Verlag, Berlin, 1988.

- [18] M. DOROBANTU AND B. ENGQUIST, *Wavelet-based numerical homogenization*, SIAM J. Numer. Anal., 35 (1998), pp. 540–559.
- [19] J. DOUGLAS JR AND T. DUPONT, *Interior Penalty Procedures for Elliptic and Parabolic Galerkin methods*, Lecture Notes in Phys. 58, Springer-Verlag, Berlin, 1976.
- [20] L. DURLOFSKY, *Numerical calculation of equivalent grid block permeability tensors for heterogeneous porous media*, Water Resources Research, 27 (1991), pp. 699–708.
- [21] W. E AND B. ENGQUIST, *The heterogeneous multiscale methods*, Commun. Math. Sci., 1 (2003), pp. 87–132.
- [22] ———, *Multiscale modeling and computation*, Notice Amer. Math. Soc., 50 (2003), pp. 1062–1070.
- [23] W. E, P. MING, AND P. ZHANG, *Analysis of the heterogeneous multiscale method for elliptic homogenization problems*, J. Am. Math. Soc., 18 (2005), pp. 121–156.
- [24] Y. EFENDIEV, J. GALVIS, AND X. H. WU, *Multiscale finite element methods for high-contrast problems using local spectral basis functions*, J. Comput. Phys., 230 (2011), pp. 937–955.
- [25] Y. EFENDIEV, V. GINTING, T. Y. HOU, AND R. EWING, *Accurate multiscale finite element methods for two-phase flow simulations*, J. Comput. Phys., 220 (2006), pp. 155–174.
- [26] Y. EFENDIEV AND T. Y. HOU, *Multiscale finite element methods theory and applications*, Springer, Lexington, KY, 2009.
- [27] Y. EFENDIEV, T. Y. HOU, AND V. GINTING, *Multiscale finite element methods for nonlinear partial differential equations*, Comm. Math. Sci., 2 (2004), pp. 553–589.
- [28] Y. EFENDIEV, T. Y. HOU, AND X. H. WU, *Convergence of a nonconforming multiscale finite element method*, SIAM J. Numer. Anal., 37 (2000), pp. 888–910.
- [29] Y. EFENDIEV AND A. PANKOV, *Numerical homogenization of nonlinear random parabolic operators*, SIAM MMS, 2 (2004), pp. 237–268.
- [30] B. ENGQUIST AND O. RUNBORG, *Wavelet-based numerical homogenization with applications*, in Multiscale and Multiresolution Methods: Theory and Applications, T. Barth, T. Chan, and R. Heimes, eds., vol. 20 of Lecture Notes in Computational Sciences and Engineering, Springer-Verlag, Berlin, 2002, pp. 97–148.
- [31] C. FARHAT, I. HARARI, AND L. P. FRANCA, *The discontinuous enrichment method*, Comput. Meth. Appl. Mech. Eng., 190 (2001), pp. 6455–6479.
- [32] C. L. FARMER, *Upscaling: A review*, in Proceedings of the Institute of Computational Fluid Dynamics Conference on Numerical Methods for Fluid Dynamics, Oxford, UK, 2001.

- [33] X. FENG AND H. WU, *Discontinuous Galerkin methods for the Helmholtz equation with large wave numbers.*, SIAM J. Numer. Anal., 47 (2009), pp. 2872–2896, also downloadable at <http://arXiv.org/abs/0810.1475>.
- [34] ———, *hp-discontinuous Galerkin methods for the Helmholtz equation with large wave number*, Math. Comp., (2011, posted online).
- [35] J. FISH AND V. BELSKY, *Multigrid method for a periodic heterogeneous medium, part i: Multiscale modeling and quality in multidimensional case*, Comput. Meth. Appl. Mech. Eng., 126 (1995), pp. 17–38.
- [36] J. FISH AND Z. YUAN, *Multiscale enrichment based on partition of unity*, Inter. J. Numer. Meth. Eng., 62 (2005), pp. 1341–1359.
- [37] L. P. FRANCA AND A. RUSSO, *Deriving upwinding, mass lumping and selective reduced integration by residual-free bubbles*, Appl. Math. Lett., 9 (1996), pp. 83–88.
- [38] J. GALVIS AND Y. EFENDIEV, *Domain decomposition preconditioners for multiscale flows in high-contrast media*, SIAM MMS, 8 (2010), pp. 1461–1483.
- [39] ———, *Domain decomposition preconditioners for multiscale flows in high-contrast media: Reduced dimension coarse spaces*, SIAM MMS, 8 (2010), pp. 1621–1644.
- [40] D. GILBARG AND N. TRUDINGER, *Elliptic partial differential equations of second order*, Springer-Verlag, Berlin, 2001.
- [41] P. GRISVARD, *Elliptic problems on nonsmooth domains*, Pitman, Boston, 1985.
- [42] T. Y. HOU AND X. H. WU, *A multiscale finite element method for elliptic problems in composite materials and porous media*, J. Comput. Phys., 134 (1997), pp. 169–189.
- [43] T. Y. HOU, X. H. WU, AND Z. CAI, *Convergence of a multiscale finite element method for elliptic problems with rapidly oscillation coefficients*, Math. Comp., 68 (1999), pp. 913–943.
- [44] T. Y. HOU, X. H. WU, AND Y. ZHANG, *Removing the cell resonance error in the multiscale finite element method via a petrov-galerkin formulation*, Commun. Math. Sci., 2 (2004), pp. 185–205.
- [45] T. HUGHES, *Multiscale phenomena: Green’s functions, the dirichlet to neumann formulation, subgrid scale models, bubbles and the origin of stabilized methods*, Comput. Meth. Appl. Mech. Eng., 127 (1995), pp. 387–401.
- [46] P. JENNY, S. LEE, AND H. TCHELEPI, *Multi-scale finite-volume method for elliptic problems in subsurface flow simulation*, Journal of Computational Physics, 187 (2003), pp. 47–67.
- [47] V. V. JIKOV, S. M. KOZLOV, AND O. A. OLEINIK, *Homogenization of differential operators and integral functionals*, Springer-Verlag, Berlin, 1994.

- [48] R. MASSJUNG, *An hp-error estimate for an unfitted discontinuous Galerkin method applied to elliptic interface problems*, RWTH 300, IGPM Report, 2009.
- [49] S. MOSKOW AND M. VOGELIUS, *First-order corrections to the homogenised eigenvalues of a periodic composite medium. a convergence proof*, PROCEEDINGS-ROYAL SOCIETY OF EDINBURGH A, 127 (1997), pp. 1263–1300.
- [50] J. D. MOULTON, J. E. DENDY, AND J. M. HYMAN, *The black box multigrid numerical homogenization algorithm*, J. Comput. Phys., 141 (1998), pp. 1–29.
- [51] H. OWHADI AND L. ZHANG, *Metric-based upscaling*, Communications on pure and applied mathematics, 60 (2007), pp. 675–723.
- [52] ———, *Localized bases for finite-dimensional homogenization approximations with non-separated scales and high contrast*, SIAM Multiscale Modeling and Simulation, 9 (2011), pp. 1373–1398.
- [53] M. PESZYŃSKA, M. WHEELER, AND I. YOTOV, *Mortar upscaling for multiphase flow in porous media*, Computational Geosciences, 6 (2002), pp. 73–100.
- [54] G. SANGALLI, *Capturing small scales in elliptic problems using a residual-free bubbles finite element method*, SIAM Multiscale Model. Simul., 1 (2003), pp. 485–503.
- [55] R. SCOTT AND S. ZHANG, *Finite element interpolation of nonsmooth functions satisfying boundary conditions*, Mathematics of Computation, 54 (1990), pp. 483–493.
- [56] M. F. WHEELER, *An elliptic collocation-finite element method with interior penalties*, SIAM J. Numer. Anal., 15 (1978), pp. 152–161.
- [57] H. WU, *Pre-asymptotic error analysis of CIP-FEM and FEM for Helmholtz equation with high wave number. Part I: Linear version*, to appear.
- [58] H. WU AND Y. XIAO, *An unfitted hp-interface penalty finite element method for elliptic interface problems*, Submitted.
- [59] X. H. WU, Y. EDENDIEV, AND T. HOU, *Analysis of hmm absolute permeability*, Discrete and Continuous Dynamical Systems-series B, (2002), pp. 185–204.
- [60] L. ZHU AND H. WU, *Pre-asymptotic error analysis of CIP-FEM and FEM for Helmholtz equation with high wave number. Part II: hp version*, to appear.